

AD 740571

AFAPL-TR-71-42

**POWER-SHARING WITH ELECTRIC PROPULSION  
AND SECONDARY BATTERIES**

*JACK W. GEIS*

TECHNICAL REPORT AFAPL-TR-71-42

DECEMBER 1971

This document has been approved for public release  
and sale; its distribution is unlimited.

REPRODUCED BY  
NATIONAL TECHNICAL  
INFORMATION SERVICE

AIR FORCE AERO PROPULSION LABORATORY  
AIR FORCE SYSTEMS COMMAND  
WRIGHT-PATTERSON AIR FORCE BASE, OHIO

87





UNCLASSIFIED  
Security Classification

DOCUMENT CONTROL DATA - R & D		
<i>(Security classification of title, body of abstract and indexing annotation must be entered when the overall report is classified)</i>		
1 ORIGINATING ACTIVITY (Corporate author) Air Force Aero Propulsion Laboratory Air Force Systems Command Wright-Patterson Air Force Base, Ohio		2a. REPORT SECURITY CLASSIFICATION UNCLASSIFIED 2b. GROUP
3 REPORT TITLE POWER-SHARING WITH ELECTRIC PROPULSION AND SECONDARY BATTERIES		
4 DESCRIPTIVE NOTES (Type of report and inclusion dates)		
5 AUTHOR(S) (First name, middle initial, last name) Jack W. Geis		
6 REPORT DATE December 1971	7a. TOTAL NUMBER OF PAGES 84	7b. NO OF REFS 22
8a. CONTRACT OR GRANT NO	9a. ORIGINATOR REPORT NUMBER(S) AFAPL-TR-71-42	
b. PROJECT NO 3141	9b. OTHER REPORT NO(S) (Any other numbers that may be assigned this report)	
c. Task No. 314102		
d.		
10 DISTRIBUTION STATEMENT This document has been approved for public release and sale; its distribution is unlimited.		
11 SUPPLEMENTARY NOTES	12 SPONSORING MILITARY ACTIVITY Air Force Aero Propulsion Laboratory Wright-Patterson Air Force Base, Ohio	
13 ABSTRACT <p>An in-house study has revealed that most AF synchronous equatorial satellites have an appreciable fraction of power on the spacecraft which is not being used continuously. The study reveals that this excess power may be used to operate electric thrusters for station-keeping functions, on an appropriate duty cycle. By selecting the proper secondary battery charge rate, commensurate with battery capacity and reliability, the electric thruster performance may be optimized to maximize satellite payload capabilities. Percent payload improvement from a few percent to 25% when compared to a non-power-sharing ion engine, and from 5 to 75% compared to a power-sharing colloid engine may be realized.</p>		

DD FORM 1473

UNCLASSIFIED  
Security Classification

AFAPL-TR-71-42

**POWER-SHARING WITH ELECTRIC PROPULSION  
AND SECONDARY BATTERIES**

*JACK W. GEIS*

This document has been approved for public release  
and sale, its distribution is unlimited.

AFAPL-TR-71-42

FOREWORD

The analysis reported herein was performed as an in-house effort by the author for the Aerospace Power Division, Air Force Aero Propulsion Laboratory, Wright-Patterson Air Force Base, Ohio. The work was accomplished under Task 314102, Project 3141, "Electric Propulsion Technology." The analysis was conducted from November 1970 to April 1971.

The report was submitted by the author 30 April 1971.

This report has been reviewed and is approved.



ROBERT G. SURETTE, Major, USAF  
Chief, Laser & Aircraft  
Power Branch

ABSTRACT

An in-house study has revealed that most AF synchronous equatorial satellites have an appreciable fraction of power on the spacecraft which is not being used continuously. The study reveals that this excess power may be used to operate electric thrusters for stationkeeping functions, on an appropriate duty cycle. By selecting the proper secondary battery charge rate, commensurate with battery capacity and reliability, the electric thruster performance may be optimized to maximize satellite payload capabilities. Percent payload improvement from a few percent to 25% when compared to a non-power-sharing ion engine, and from 5 to 75% compared to a power-sharing colloid engine may be realized.

## TABLE OF CONTENTS

SECTION	PAGE
I INTRODUCTION	1
II SPACE POWER CHARACTERISTICS THROUGH POWER SHARING	3
1. Energy Storage With Secondary Batteries	3
2. Power Profile	3
3. Battery Charge Rate	3
4. Solar Panel Sizing	8
5. Summary of Space Power Characteristics Through Power Sharing	10
III ELECTRIC PROPULSION CHARACTERISTICS THROUGH POWER SHARING	16
1. Power Sharing on a DOD Satellite	16
2. Highly Energetic Near-Earth Missions	17
3. Thruster Duty Cycle for N/S Station Keeping in a Synchronous Equatorial Orbit	19
4. Redundancy Considerations	21
IV PERFORMANCE TRADEOFFS REALIZED BY POWER SHARING	23
V CONCLUSIONS AND RECOMMENDATIONS	40
APPENDIX I BATTERY ANALYSIS	42
APPENDIX II PROPULSION AND POWER PERFORMANCE CONSTRAINTS	61
APPENDIX III POSITION OF THE NODES FOR A SYNCHRONOUS EQUATORIAL ORBIT	63
APPENDIX IV DIGITAL COMPUTER PROGRAM FOR POWER-SHARING ANALYSIS	68
REFERENCES	71

## LIST OF ILLUSTRATIONS

FIGURE		PAGE
1.	Relative Position of a Satellite in Synchronous Equatorial Orbit With Respect to the Earth's Shadow	4
2.	Power Profile for a Synchronous Equatorial Satellite	5
3.	Influence of Secondary Battery Charge Rate on Power Profile	7
4.	Solar Array/Load Battery Interface Diagram	9
5.	Maximum Power Degradation for N/P, 10-Ohm -Cm Silicon Cells Versus Time in Synchronous Orbit	11
6.	Solar Panel Subsystem Performance Trends	12
7.	Influence of Battery Charge Rate and Array Degradation on Solar Panel Sizing	13
8.	Electrical Power System Block Diagram	14
9.	N/S Perturbations on Synchronous Equatorial Orbits	18
10.	Uncorrected Latitudinal Satellite Motion	18
11.	Velocity Increment per Year for Secular North-South Station Keeping as a Function of Duty Cycle	20
12.	Isp Values Selected for the Ion Engine Systems	25
13.	Calculated Weights for Different Thruster Systems	28
14.	System Performance for Bombardment Ion Engine of Millipound Thrust Size	30
15.	Secondary Battery/Solar Panel System Weight Tradeoffs as a Function of Battery Charge Rate, With Solar Panel $\alpha$ sp = 100 lbs/kw	32
16.	Secondary Battery/Solar Panel System Weight Tradeoffs as a Function of Battery Charge Rate, With Solar Panel $\alpha$ sp = 50 lbs/kw	33
17.	Payload Improvement of Ion Thrusters Using Full and Partial Power Sharing, Versus Non-Power-Sharing Ion Engine	34
18.	Payload Improvement of Ion Thruster Using Full and Partial Power Sharing, vs 1500 Sec Colloid Thruster with Power Sharing	35

## LIST OF ILLUSTRATIONS (Contd)

FIGURE		PAGE
19.	Payload Improvement of Ion Thruster Using Full and Partial Power Sharing, vs 2000 Sec Colloid Thruster Using Full Power Sharing	36
20.	Payload Improvement Realized With Power Sharing as a Function of Mission Time	37
21.	Payload Improvement Realized With Power Sharing as a Function of Mission Time	38
22.	Influence of Depth of Discharge on Battery Specific Weight	43
23.	Critical Charge Voltage as a Function of Cell Temperature and Charge Rate	45
24.	Available Capacity Vs Temperature	46
25.	Cell Voltage as a Function of Cell Temperature and Battery Charge Rate	47
26.	Influence of Charge Rate and Temperature on Recharge Efficiency	48
27.	Influence of Battery Temperature on Cycle Life	50
28.	Cycle Life of Ni-Cd Cells	51
29.	Influence of Charge Rate on Battery Cycle Life	52
30.	Influence of Battery Charge Rate and Cell Stringing on Cell String Reliability	53
31.	Voltage Limit, Constant Current Charge Control, With Current-Initiated Switchdown	56
32.	Comparison of Charge Control Methods	57
33.	Thruster/ Battery Charging Operating Cycles for Synchronous Equatorial Satellite During 45-Day Autumnal Equinox Season	64
34.	Typical Power Profile for Synchronous Equatorial Satellite With C/4 Battery Charge Rate, During Autumnal Equinox	66
35.	Typical Power Profile for Synchronous Equatorial Satellite With C/10 Battery Charge Rate During Autumnal Equinox	67

AFAPL-TR-71-42

LIST OF TABLES

TABLE		PAGE
I	Synchronous Equatorial Satellite Performance Characteristics	26
II	Satellite Power Budget for N/S Station Keeping	29

SECTION I  
INTRODUCTION

In the last few years, certain electric propulsion systems have progressed technically to the point where they are being seriously considered for application on near-earth satellites. Advanced Development Plans and space demonstrations are planned and programmed to establish long-term reliability of electric propulsion systems and their capability to perform functions such as station keeping, altitude control, initial station acquisition, repositioning, drag cancellation, and elimination of rotation of the line of apsides of an elliptical orbit.

All electric thrusters require power to generate a plasma or ionized gas and to accelerate this gas to high velocities so as to produce thrust. The specific impulse at which these engines operate varies from the medium-to-high range (2500 to 10,000 seconds) for the ion engine, to the low range (which varies from 500-600 seconds at the lower end of the range to 1500-2000 seconds at the upper end) for the colloid engine. Pulsed plasma devices use energy-storing techniques, such as capacitor banks and can operate across a broad range of specific impulse, as low as the colloid or as high as the ion engine.

Electric power on board satellites, particularly the high-altitude satellites, is generally at a premium. Panel and body-mounted solar cells have been used to supply electrical power for spacecraft. The number of body-mounted cells is limited, however, by the useful surface area of the spacecraft, and solar panels could become unwieldy since they would be increased approximately  $1 \text{ ft}^2$  (1/2 to 1 lb weight) for every 10 watts.

The performance of electric thrusters (that is, their thrust and Isp level) is a strong function of satellite weight, mission lifetime, and available power. In order to minimize total system weight, the specific impulse of the electric thruster should be optimized, consistent with the reliability of the thruster system. As mission times and satellite weights increase, and more energy mission functions are performed, the specific impulse and thrust level must also increase.

AFAP1-TR-71-42

Without adequate power, many missions cannot be optimized in terms of minimum satellite weight. A satellite can be designed that trades off increased solar panel size and weight with reduced thruster propellant weight to produce minimum system weight. To do this, the satellite designer must consider electric propulsion needs and requirements at design inception, but this has been difficult to do because of insufficient information on electric thruster reliability. Air Force and NASA advanced and exploratory development programs, however, are providing improved confidence in electric engines. Even if no additional solar panels are added to provide power for electric propulsion, power sharing should make it possible to more completely optimize electric thruster performance.

## SECTION II

### SPACE POWER CHARACTERISTICS THROUGH POWER SHARING

#### 1. ENERGY STORAGE WITH SECONDARY BATTERIES

Most near-earth and synchronous-orbit satellites spend some time in the Earth's shadow. This amount of time may range from 35 minutes in a 90-minute near-earth orbit to 72 minutes during the eclipse season of a synchronous equatorial orbit. Figure 1 shows the dark time experienced by a synchronous satellite during a year. Military philosophy requires satellite electrical equipment (communication, surveillance, etc.) to be operated 100% of the time; since solar cells require sunlight to generate power, some means must be found for storing electrical energy so that it is available during the dark time.

A secondary battery\* can store energy collected by the solar cells during the daylight period and discharge it during the dark time. As the satellite enters another daylight period, the solar cells collect enough energy to recharge the battery, which can then be used during the next dark time.\*\*

#### 2. POWER PROFILE

A typical power profile is shown in Figure 2 for a maximum eclipse period for a 24-hour orbit. The power load to the electronics on the spacecraft must be held constant, so that the spacecraft is 100% functional at all times. Therefore, the solar panel array must be sized so that sufficient power is generated during the light period to recharge the batteries.

#### 3. BATTERY CHARGE RATE

A certain amount of solar power is demanded for battery recharging. Consider a battery which has a capacity of  $C = 100$  AH. If the battery is

---

\* Secondary battery: Capable of many charge-discharge cycles, in contrast to primary battery which can be discharged only one time.

\*\* Regenerative fuel cells have not been considered in this study. A similar study should be made with these energy storage devices when performance and reliability data become more readily available.

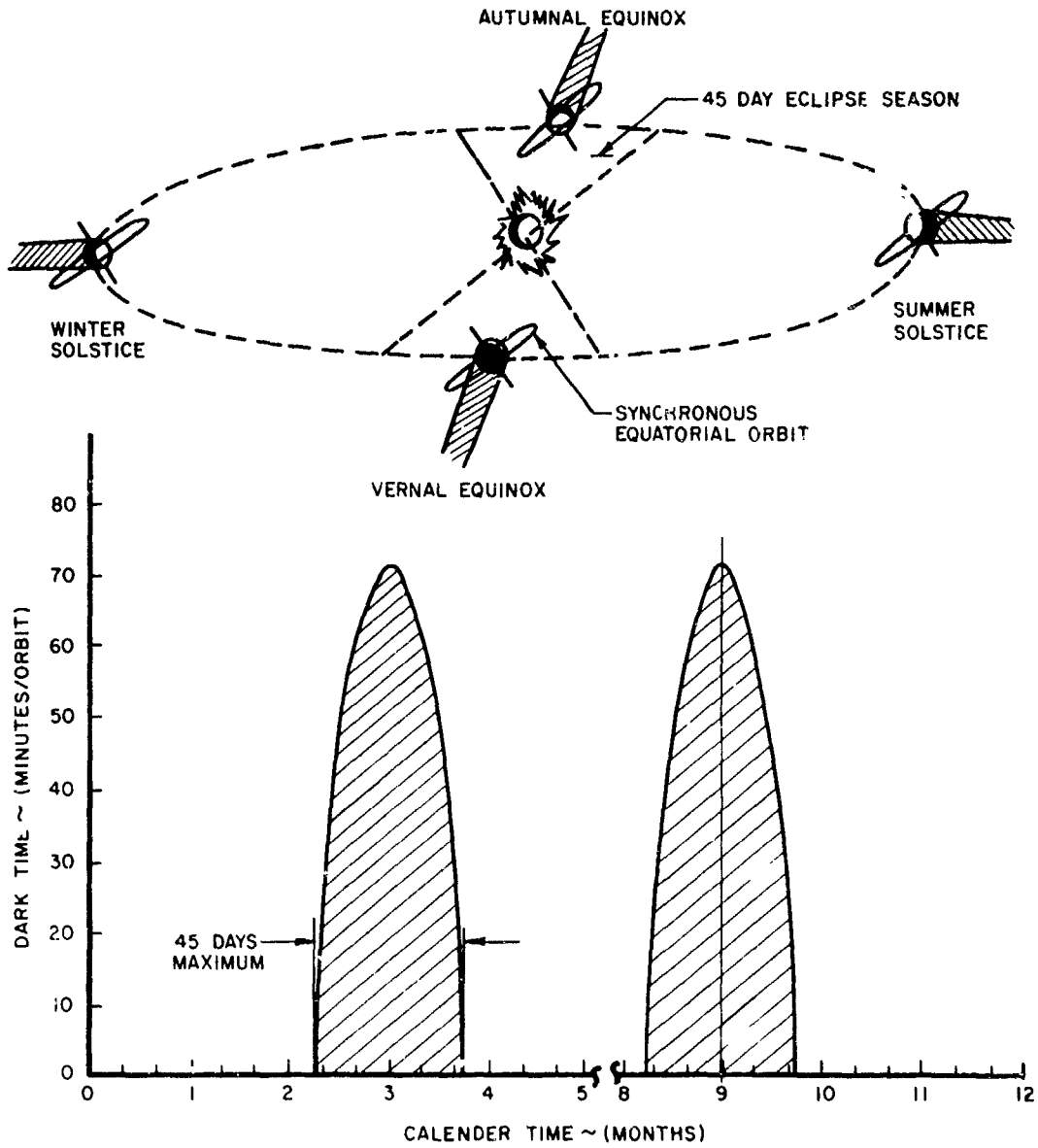


Figure 1. Relative Position of a Satellite in Synchronous Equatorial Orbit With Respect to the Earth's Shadow

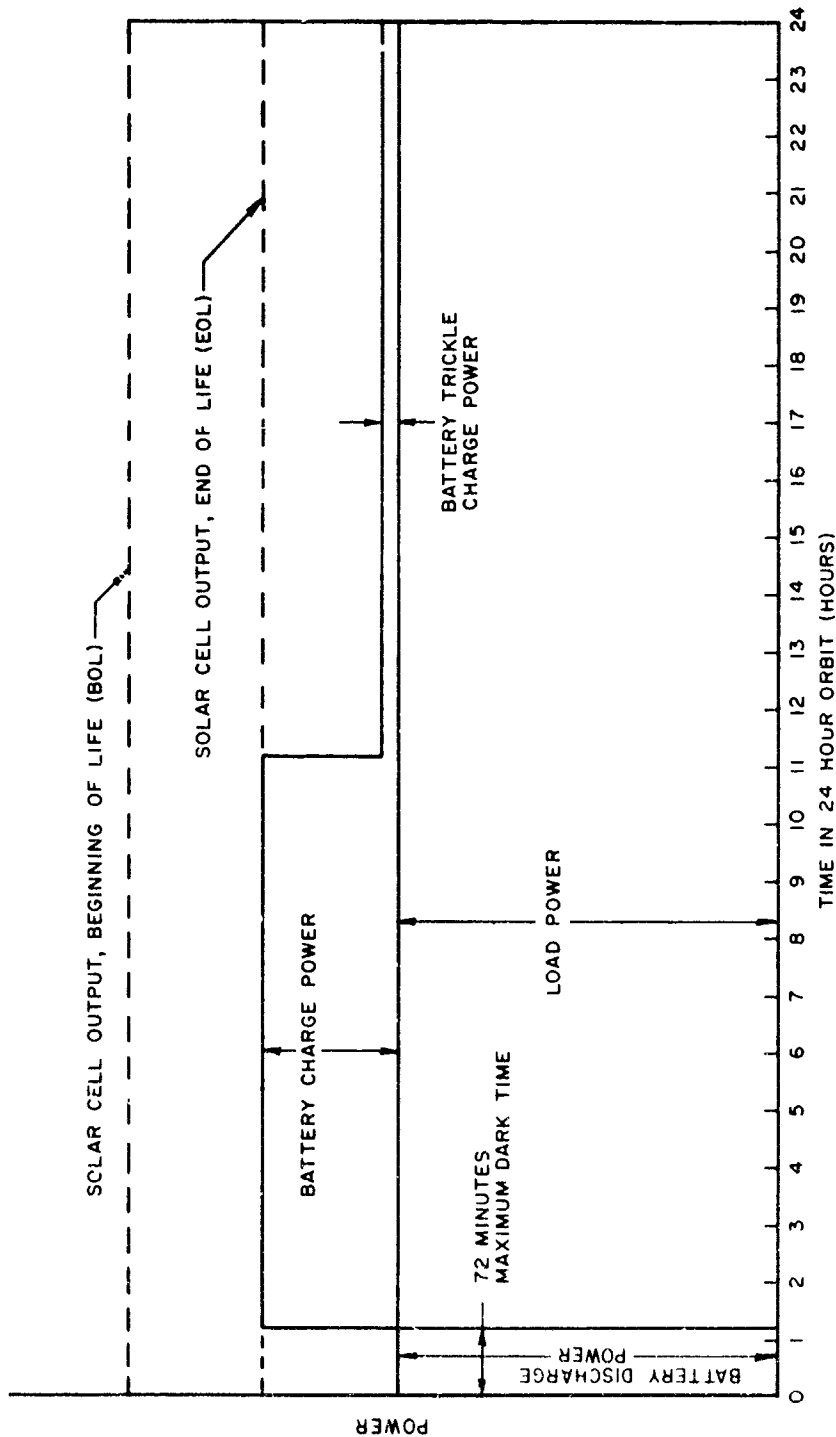


Figure 2. Power Profile for a Synchronous Equatorial Satellite

recharged at a bus voltage of 30 volts, and a charge rate of  $C/10 = 10$  amps, then the instantaneous power required is  $30V \times 10 \text{ amps} = 300$  watts. Charging at a slower rate, say  $C/25 = 4$  amps, would require only  $30 \times 4 = 120$  watts. In terms of minimizing solar panel size and weight, therefore, the battery should be charged at a slow rate.

The minimum time available to recharge a battery on a synchronous, equatorial satellite where the maximum eclipse time is 72 minutes would be 24 hours -  $72/60 = 22.8$  hours. The required charge current for a 100 AH battery would then be

$$I = \frac{(AH) (\% \text{ D.O.D.}) (\% \text{ overcharge})}{t_{\text{charge}} (10^4)}, \text{ amperes} \quad (1)$$

where % D.O.D. = % depth of discharge, or proportion of nominal capacity removed from a cell during each discharge cycle,  $\frac{\text{ampere-hours removed} \times 100}{\text{ampere-hours capacity}}$ ,  
 % overcharge = amount of electrical energy put in to fully recharge the battery, in % =  $\frac{AH \text{ input during charge} \times 100}{AH \text{ capacity}}$

For an 80% D.O.D and overcharge of 120%, the current required to recharge a 100 AH battery with a charge time of 22.8 hours is  $I = \frac{100 (.80) (1.20)}{22.8} = 4.2$  amps. The charge rate, thus, would be  $C/100/4.2 = C/23.8$ .

The question that now comes to mind is: Is it desirable from the standpoint of overall satellite power, weight constraints, and battery reliability to always charge at the lowest possible rate? Certain advantages could be gained on the overall satellite system weight if it is feasible to charge at a faster rate.

Figure 3 shows the effect of the recharging rate on the power budget. Some of the power from the solar array is not used 100% of the time at the faster recharging rate because the battery charge time does not extend over the entire light time. For an 80% D.O.D and 120% overcharge, a  $C/10$  charge rate would fully recharge the battery in 9.6 hours; this would leave 13.2 hours of light time when the power from the solar panel could be used for something other than recharging the battery. This power is not used on current spacecraft

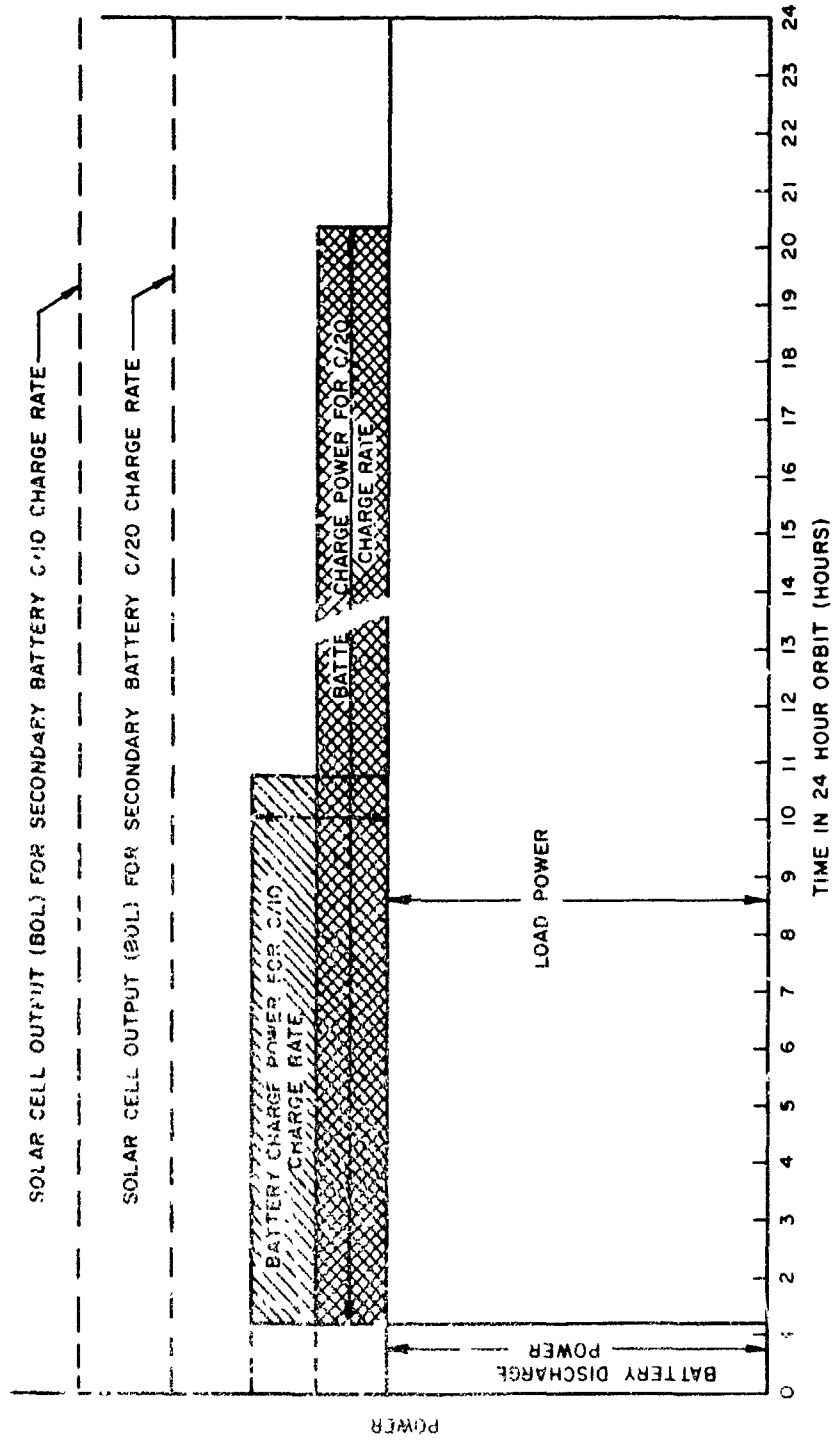


Figure 3. Influence of Secondary Battery Charge Rate on Power Profile

because the solar panel is sized to charge the battery, and the power load for the equipment on the satellite is already part of the power budget (see Figure 2 or 3). Since this excess power is not needed after the secondary battery is fully recharged it is directed away through a shunt voltage limiter, which thermally dissipates it. This dissipated power could be used for transient loads of millisecond duration, such as antenna slewing or command processing; for downlink telemetry loads, which may exist for as long as 5 hours; or for supplying, in combination with the recharged battery, peak power needed for emergency loads. Emergency conditions should be rare, but if the battery is recharged at a sufficiently fast rate, power from both the solar panel and the battery will be available over a considerable portion of the orbit.

Unless some technical objections to charging the battery at a faster rate exist, a certain amount of solar power should be available (25-50% of each synchronous equatorial orbit), which may be used to power an electric thruster for such useful functions as station keeping. The specific tradeoffs in terms of total power/propulsion system weights will be discussed in Section IV of this report. The factors influencing the selection of a battery charge rate and charge detection and control techniques are discussed in Appendix I.

#### 4. SOLAR PANEL SIZING

Solar panels on a spacecraft must be sized to charge the batteries and to provide load power throughout the mission (see Figure 2); thus, power output degradation must be considered. Degradation occurs over a period of years, and the array must be sized to deliver the required load power to the end of the mission (end of life, EOL). Many conditions, including the trapped electron environment of the synchronous orbit and the proton environment of a solar flare or a nuclear blast, contribute to the degradation of electrical output of these cells (Reference 1, page 51).

A typical interface diagram of a solar array/battery load is shown in Figure 4. The line for constant power load is seen to pass under the solar array I/V line. The area labeled "excess current available for battery charge" results from sizing the battery to take care of power demands for both constant loads and battery charging. The solar array I/V characteristic degrades with

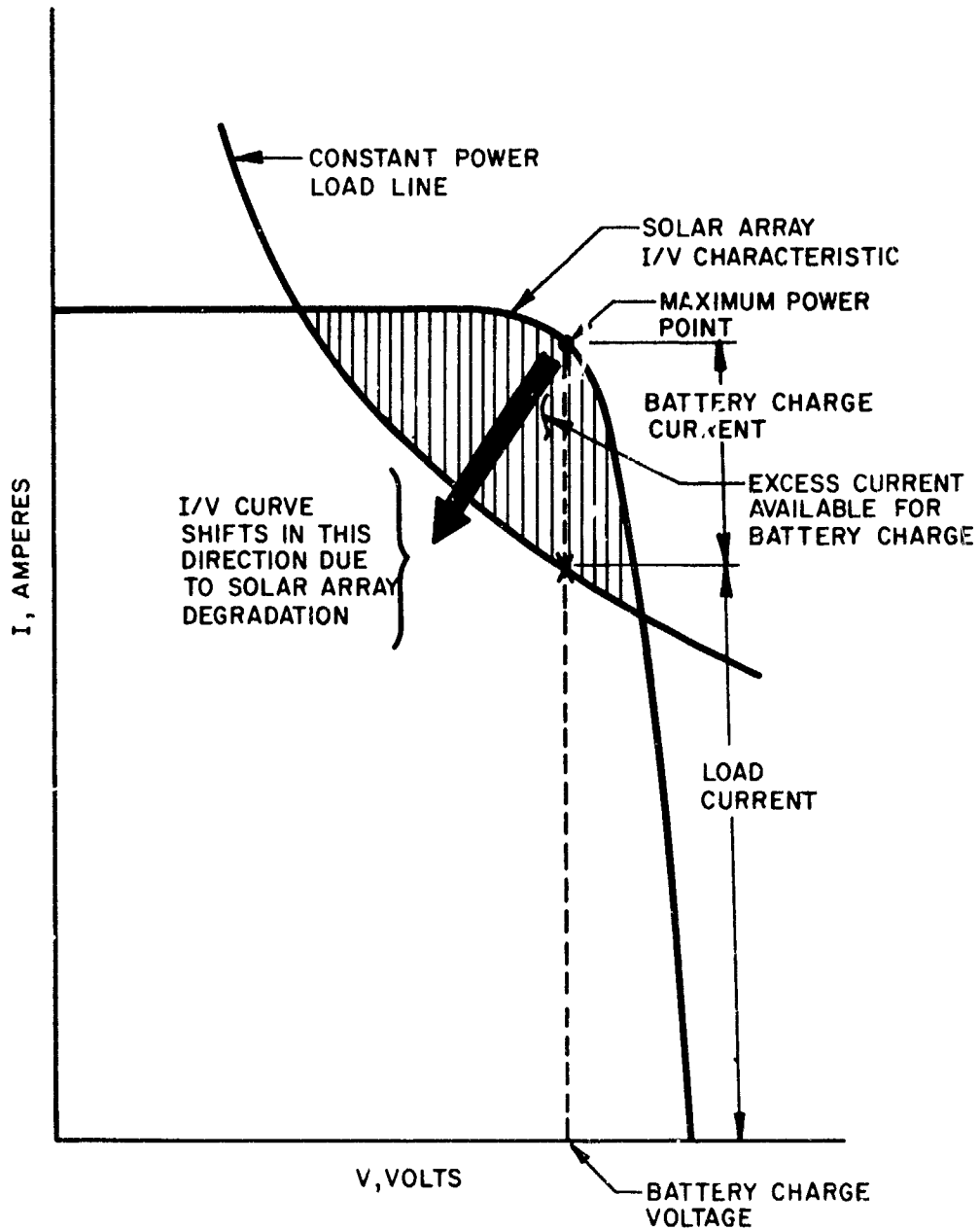


Figure 4. Solar Array/Load Battery Interface Diagram

time, which makes less power available for battery charging. If the array has been sized to charge the battery at some minimum rate, the excess power will never drop below this minimum level. Early in the life of the spacecraft, therefore, the battery may be charged at a somewhat higher rate. The electric thruster could use the excess power early in the mission for operating at a higher performance level on a selected duty cycle.

The degradation of power as a function of time is shown in Figure 5 for contemporary 10 ohm-cm N/P silicon solar cells. Degradation of solar cells is highly variable and unpredictable, however, so this curve represents a conservative estimate. New solar cell materials and design, of course, may reduce this degradation.

The specific weight of solar panels has been calculated to be approximately 50-75 lbs/kw (20-13 watts/lb, B.O.L) for flexible kw-size arrays (Reference 1, page 17). This includes the weight of the solar cells and the substrate, but not of the wiring or the support structure for extending the panels. This trend toward lighter arrays is shown in Figure 6 (Reference 2). The effect of varying battery charge rate on solar panel power is shown in Figure 7.

A typical block diagram of a solar array/battery subsystem is shown in Figure 8.\* The exact configuration selected for a synchronous satellite will depend on factors such as component weight, complexity, and reliability.

## 5. SUMMARY OF SPACE POWER CHARACTERISTICS THROUGH POWER SHARING

Fast charging provides the following advantages and disadvantages:

### a. Disadvantages

- (1) Increases size and weight of solar array.
- (2) Requires more precise overcharge sensing and control.

\* Most arrays operate with an unregulated bus. The voltage range is determined by the minimum battery voltage and by a voltage limiter at the maximum battery voltage (Reference 3, page 142). As part of the load power is taken out of the circuit, the shunt regulator comes on when the array voltage begins to rise above a certain limit. If the bus voltage is below that required to efficiently charge the battery, then a boost regulator is required to step up the voltage.

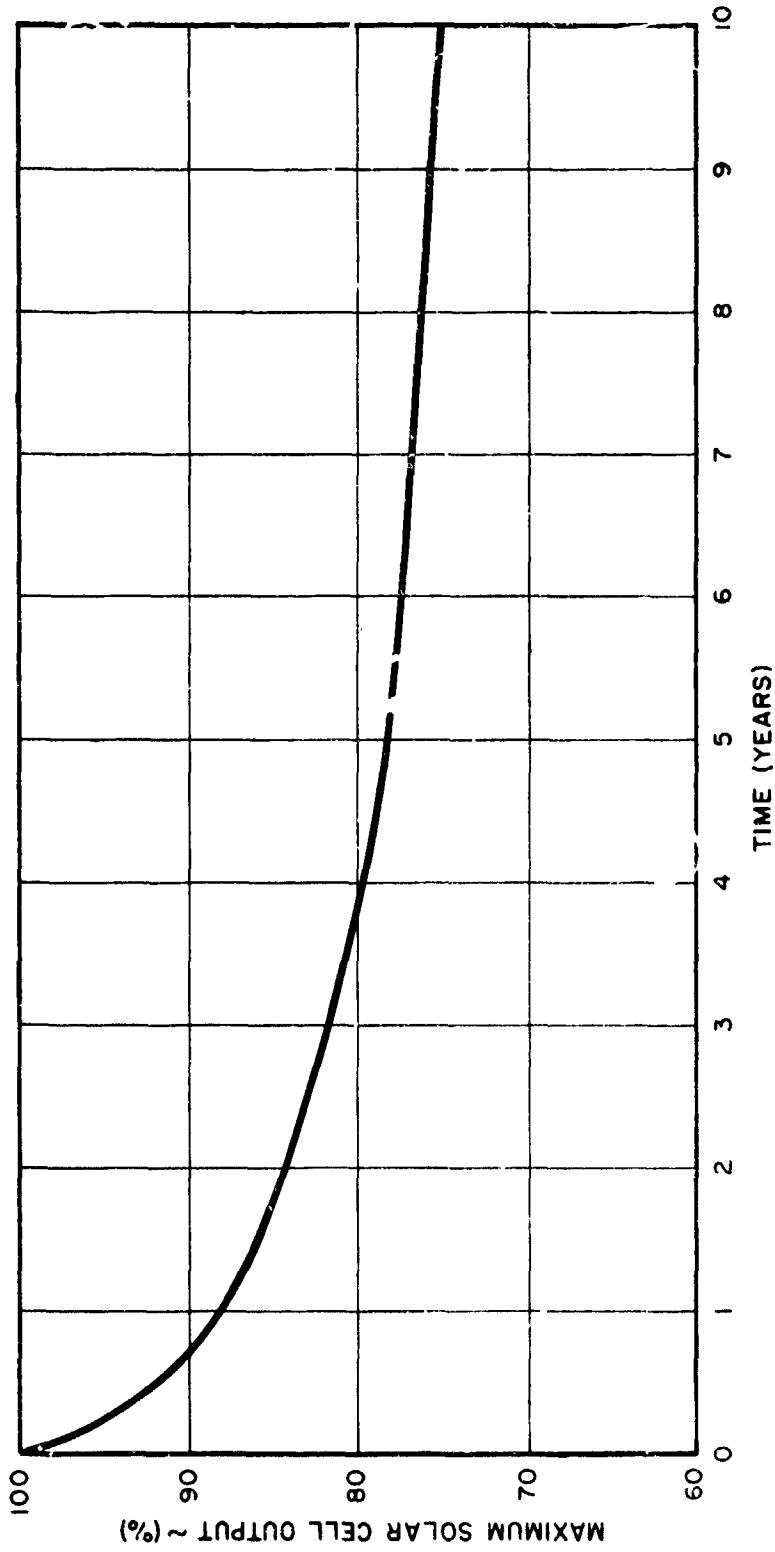


Figure 5. Maximum Power Degradation for N/P, 10-Ohm -Cm Silicon Cells Versus Time in Synchronous Orbit

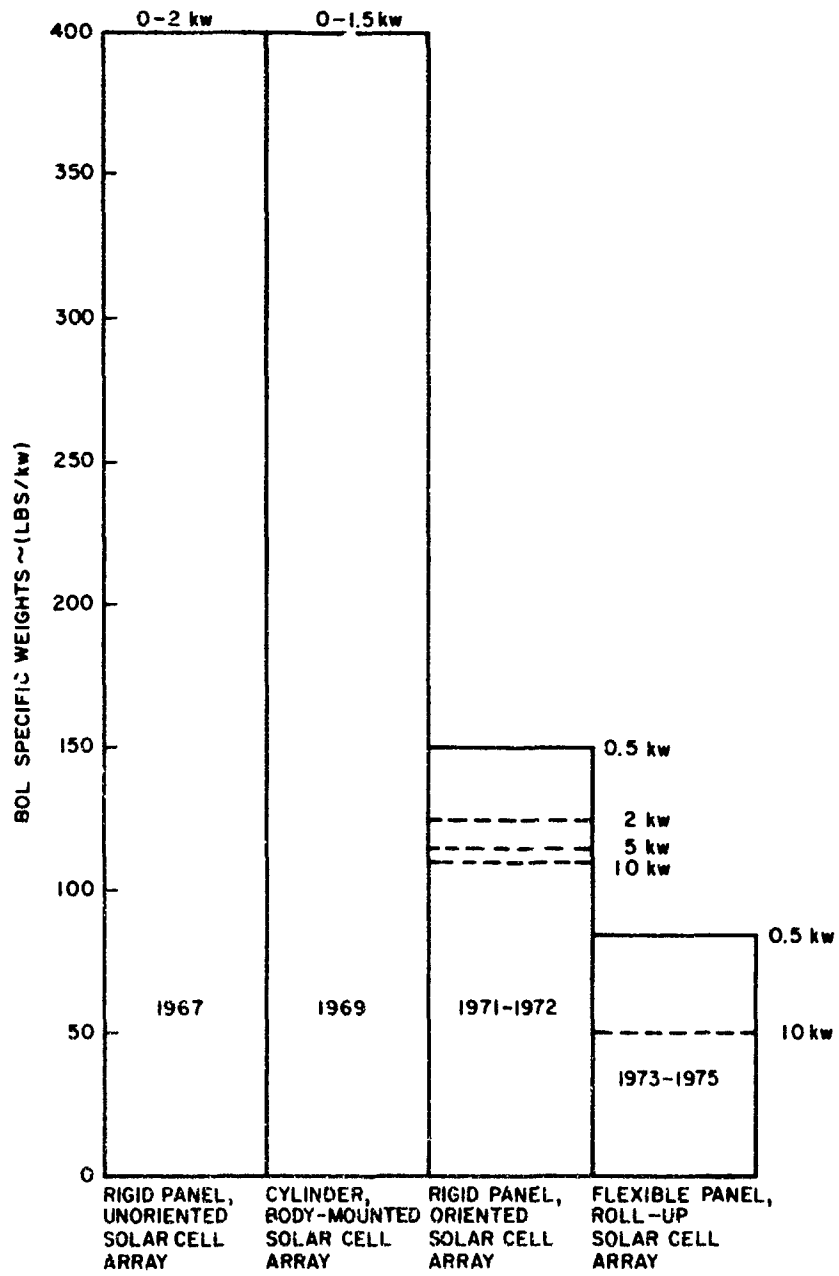


Figure 6. Solar Panel Subsystem Performance Trends

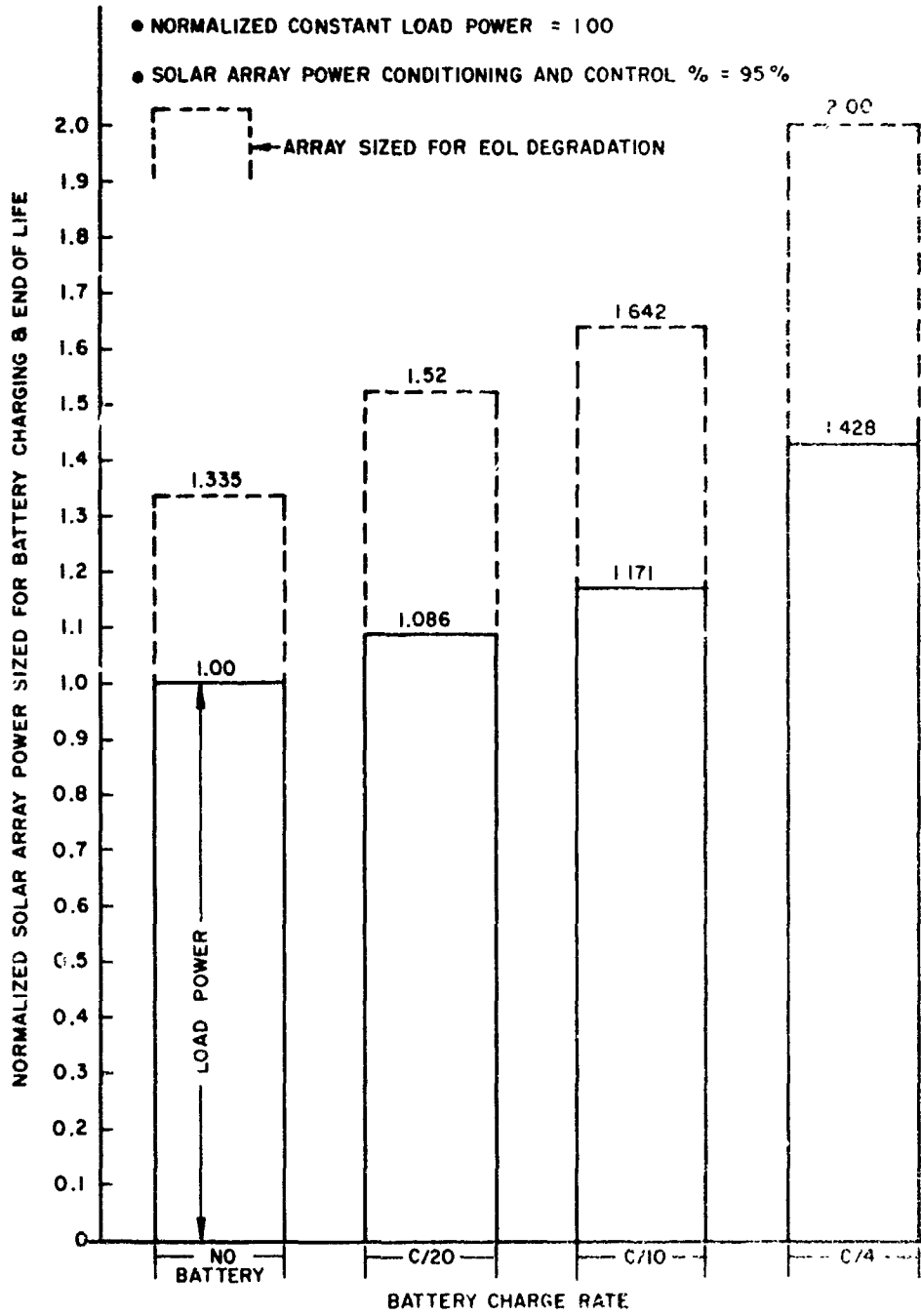


Figure 7. Influence of Battery Charge Rate and Array Degradation on Solar Panel Sizing

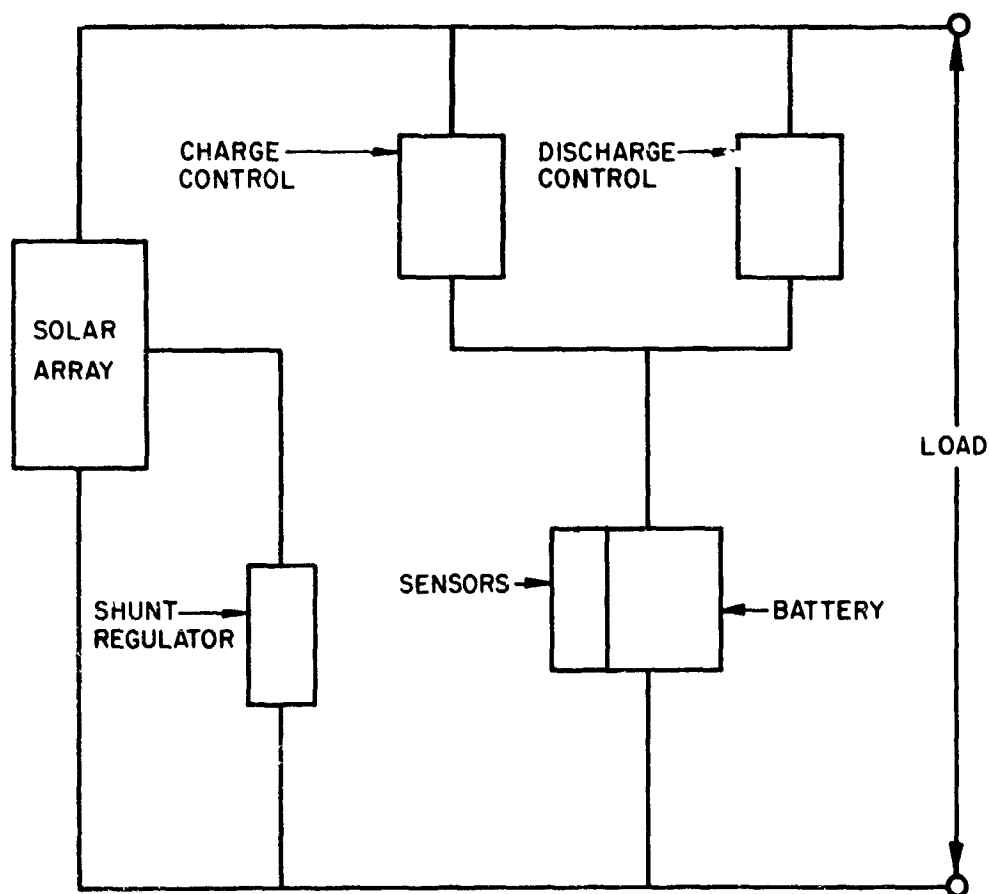


Figure 8. Electrical Power System Block Diagram

AFAPL-TR-71-42

(3) Increases heat load during battery overcharging.

(4) Battery system reliability is largely dependent on the reliability of the overcharge detection system.

b. Advantages

(1) Maintains higher battery capacity.

(2) Data indicates reliability enhanced by increased charge rate; battery size and weight reduced because of less redundancy and higher battery capacity. (Sequential charging provides little or no advantage and adds complexity.)

(3) Increases utility of secondary batteries by making possible applications where long recharging times are intolerable (such as in the early warning satellite).

(4) Overall battery/solar panel/thruster station-keeping weights can decrease significantly if battery charging rate is optimized in the approximate range of  $C/4$  to  $C/10$ .

## SECTION III

## ELECTRIC PROPULSION CHARACTERISTICS THROUGH POWER SHARING

## 1. POWER SHARING ON A DOD SATELLITE

Many factors influence the decision of whether or not to power share on a satellite. As discussed in Appendix I, battery reliability as a function of charge rate and solar array sizing play a prime roll in this decision.

Analyses for power sharing on satellites that require only a few years operational life and nominal station-keeping functions indicate only small performance tradeoffs. If the total impulse requirement is small enough that it can be satisfied with a chemical thruster and the thruster system weight including propellant is only a small fraction of the spacecraft weight, electric propulsion would not show a significant advantage, even with power sharing. It is on missions having a  $\Delta V^*$  requirement on the order of several hundred feet/sec/year or more, with mission times approaching 5-10 years, where power sharing comes into its own. Simple mission analyses show optimum specific impulse values would exceed the 1500-2000 sec capability of the colloid engines. These missions can be accomplished effectively only if sufficient power is on board for the electric thruster, or if solar power can be made available through sharing with the secondary batteries on a proper duty cycle. Propellant for performing the different station-keeping functions is the major weight fraction of the electric thruster system for these missions. The optimum Isp increases as the solar panel specific weight decreases and total thrust time increases. For several reasons, including reliability and obsolescence of the near-earth spacecraft equipment, mission times probably will not exceed 10 years. Performance gains can be realized by increasing mission time out to 10 years, but large gains from operating at high Isp require energetic missions (requiring  $> 200$  ft/sec/year) where sufficient solar power is available for sensors, battery charging, etc., and an appreciable fraction of this power can be used by the electric thruster on a noninterfering duty cycle.

$$^* \frac{\Delta V}{yr} = \text{characteristic velocity increment/yr} \sim \frac{\text{mission total impulse}}{\text{satellite mass} \times \text{year}}, \text{ in } \frac{\text{ft}}{\text{sec-yr}}$$

In summary, the following factors must be considered in determining whether or not a mission should use power sharing:

a. Requirements for highly precise satellite control (high  $\Delta V$ ) as opposed to letting the satellite drift, or using nodding antennas to compensate for satellite drift.

b. Duration of mission.

c. Sufficient power on board so that the electric thruster can optimize Isp by taking advantage of the excess power; this analysis is considered to demand a load power of 1 watt per pound of satellite weight.

## 2. HIGHLY ENERGETIC NEAR-EARTH MISSIONS

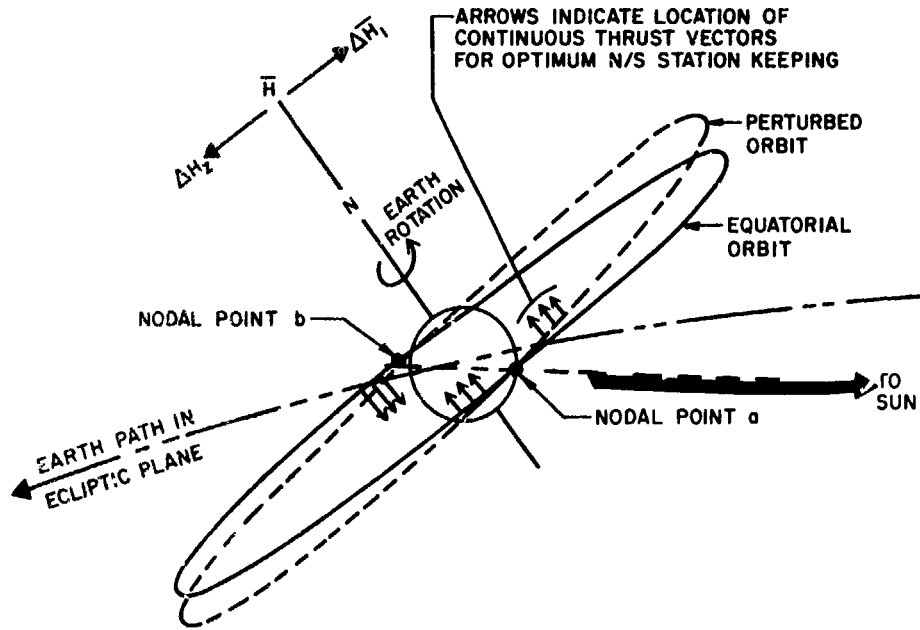
We will constrain this analysis to military missions that demand a constant load power to the spacecraft sensor\*. This means that during eclipse periods, batteries must be used to maintain the constant load power.

Perturbation effects due to the sun, moon, and the earth's asphericity can cause satellites in a synchronous equatorial orbit to drift out of station: in-track (E/W), out-of-track (N/S), and in-track radially. The largest perturbation is the N/S drift (see Figure 9). The energy requirement for "secular" N/S station keeping is about 150 ft/sec/year. If we consider perturbations that cause short-term or "diurnal" effects with periods less than the orbital period, the energy required can be several times higher (300-700 ft/sec/yr) (References 4, 5). "Secular" or long-term perturbations cause the satellite to drift out of the orbital plane by 0.79 to 0.91 degrees/year (Figure 10). Secular station keeping limits satellite positional drift to approximately 15 NM both north and south of the original orbit (Reference 6). The apparent motion of the satellite on the surface of the earth describes a figure "8", with the center of the "8" in the equatorial plane and the top and bottom north and south of the plane.

---

\* Power sharing may also be performed during initial station acquisition or satellite repositioning, when the satellite sensors are not functioning.

- $\bar{H}$  : ANGULAR MOMENTUM VECTOR DUE TO EARTH ROTATION
- $\Delta H_1$  : MOMENTUM VECTOR DUE TO LUNAR-SOLAR PERTURBATION OF ORBIT INCLINATION
- $\Delta H_2$  : MOMENTUM VECTOR DUE TO THRUST CORRECTION MANEUVER



AUTUMNAL EQUINOX

Figure 9. N/S Perturbations on Synchronous Equatorial Orbits

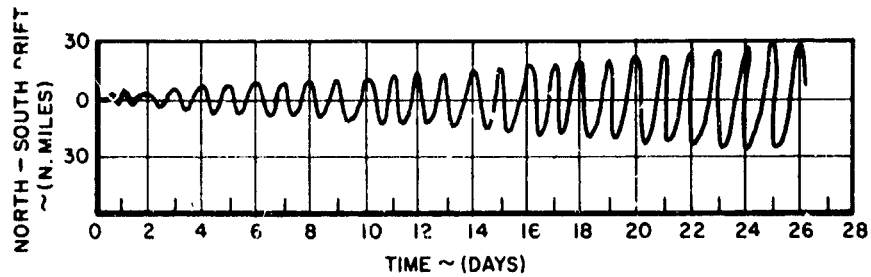


Figure 10. Uncorrected Latitudinal Satellite Motion

For navigational or data-relay satellites, very precise station keeping may be desired to allow for a very narrow spacecraft-to-spacecraft beam and to eliminate the need for complex tracking equipment both in the satellite and on the ground. Other energetic missions may involve eliminating the rotation of line of apsides, drag make-up, and spiraling (to synchronous). Eliminating the rotation of line of apsides (ERLA) can require a correction of as high as several thousand ft/sec/year, depending on the initial orbital inclination of the satellite, the eccentricity, and the desired satellite positioning.

Analyses were made of thruster system weights needed to provide station keeping, injection error removal, station acquisition, and repositioning to varying degrees. Capabilities and constraints defined for the analysis are detailed in Appendix II.

### 3. THRUSTER DUTY CYCLE FOR N/S STATION KEEPING IN A SYNCHRONOUS EQUATORIAL ORBIT

To maintain the satellite in an equatorial orbit, thrusters for N/S station keeping must exert force in a direction normal to the satellite orbital plane. The engine should operate at or near the nodal points\* (see Figure 9); thrusting  $90^\circ$  away from either nodal point has no effect in counteracting the N/S perturbation (Reference 6, page 9). Because electric thrusters are power-limited, they cannot thrust impulsively at each nodal point; they must operate continuously to provide the required total impulse for correcting the orbit. Thus, some penalty is involved, and the penalty increases the longer the engine operates away from each nodal point. The effect of this penalty is shown in Figure 11. To minimize this penalty, the duty cycle for the ion engine was chosen to be no greater than 50%.

For the 24-hour synchronous orbit, two thrusters will be required. Thruster 1 will thrust in a northerly direction for 3 hours before and after crossing nodal point (a) as shown in Figure 9, and thruster 2 will thrust in a southerly direction for 3 hours before and after crossing nodal point (b). Thus the total ion engine thrust time per orbit with a duty cycle of 50% would be 12 hours.

\* Nodal points: points of intersection of the satellite orbit, and the equatorial orbit.

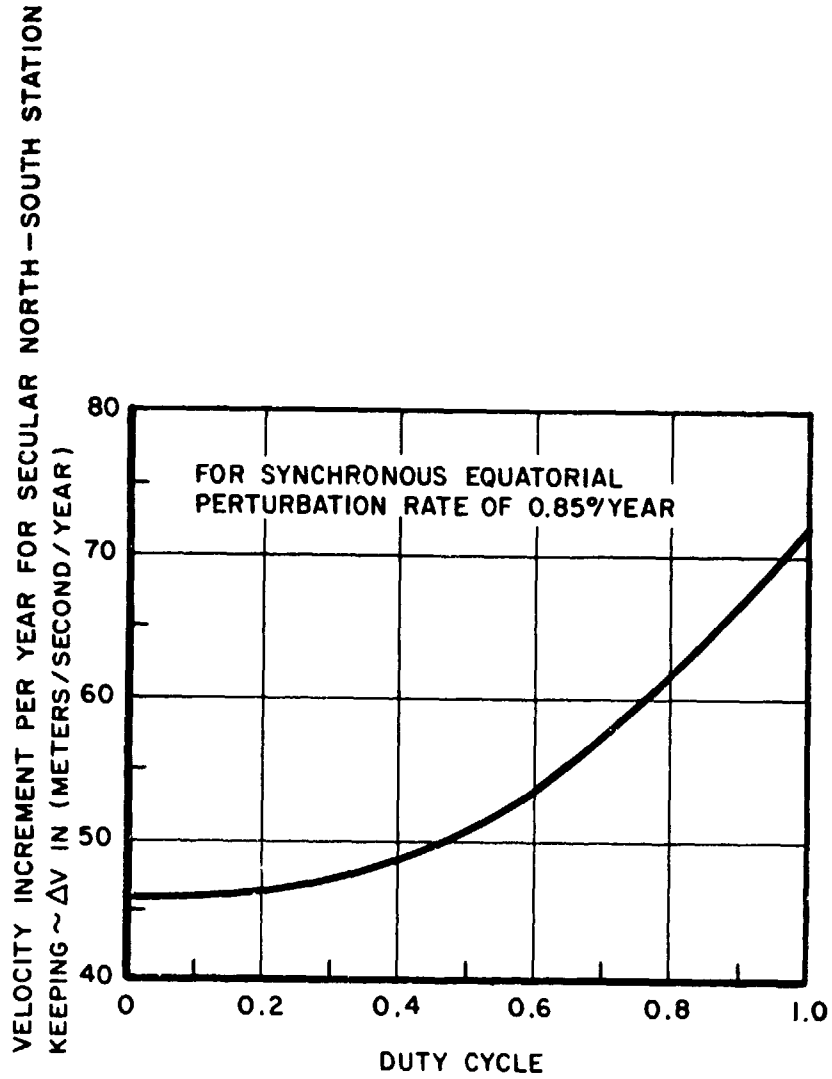


Figure 11. Velocity Increment per Year for Secular North-South Station Keeping as a Function of Duty Cycle

The duty cycle for the colloid engine was considered to be 25%, since the engine is not so severely power limited at 1500-2000 secs, although the thrust requirement has nearly doubled because of the shorter duty cycle. Therefore, each engine for N/S station keeping will operate 1-1/2 hours before and after each nodal point, for a total of 6 hours out of 24. In the weight analysis, additional weight was ascribed to the ion engine system to provide for extra thrusters to increase reliability.

#### 4. REDUNDANCY CONSIDERATIONS

For the weight analysis for missions out to 10 years, we considered the mission function to require 9 ion engines: 2 were required for N-station keeping, 2 for S-station keeping, 4 for N/S station keeping redundancy, and 1 for acquisition/repositioning maneuvers. On a 50% thruster/system duty cycle, each of the 4 prime thrusters would operate sequentially for 1.25 years during a 10-year mission.\*

We considered 5 colloid engines would be required for the 10-year mission. On a 25% thruster system duty cycle, each N-thruster and S-thruster would operate 1.25 years and each would be backed up by one redundant thruster. The fifth thruster would function as the acquisition/repositioning engine.

Power conditioning and control packages for the thrusters could be modularized and sized to operate with any thruster, including the high-thrust acquisition/repositioning thruster, at the maximum power operating point. These packages could be placed in the center of the spacecraft and isolated electrically from the thrusters.

Partial propellant feed system redundancy is achieved by using separate tanks in proximity to the N- and S-thrusters. In the event one feed system fails, half of the N/S station keeping requirements could be achieved with the remaining thruster/propellant system. The technology in feed system isolation is not very far advanced at this point, however. Exploratory

\* For the mission analysis using C/10 battery charge and  $\Delta V = 635$  ft/sec-yr, the Isp of the ion engine varied from 8500 secs to a minimum of 1820 secs near the end of the mission. Additional ion thruster weights were included because a single thruster design cannot operate across this range of Isp.

development in feed system technology for the colloid engine, which uses a liquid mixture of sodium iodide in glycerol, has developed a ladling approach toward achieving isolation. A high-voltage isolation valve isolates the thruster from the main reservoir during thruster operation. The valve is opened as necessary to transfer propellant from the main reservoir to a smaller tank. When the valve is closed, the thruster operates in electrical isolation from the other thrusters and the feed system. In the event the thruster fails [by arcing and shorting the positive high voltage source to ground], the redundant thruster can still be operated.

A high-pressure mercury-vapor isolator has been designed for use with the mercury bombardment ion engine and gas-pressurized positive-displacement feed system (Reference 7, page 73). Tests to date indicate that this concept may be satisfactory at low engine operating voltages, which occur in the 2000-3000 Isp region.

Little work has been done on feed system isolation for the cesium bombardment ion engine. This engine uses a "zero g" feed system, wherein liquid cesium is transferred by surface tension from the reservoir to the vaporizer by a network of tapered cells and a porous wick which leads from the reservoir to the vaporizer. In the vaporizer the cesium is heated and passes to the engine as a gas (Reference 7, page 19). A cesium high voltage isolator would have to be placed in the feed line downstream of the vaporizer, as is done with the mercury system. A design similar to the mercury isolator or the colloid high voltage valve/ladling concept may be feasible, but little investigation has been done. Another approach if one thruster fails may be to physically separate and seal the feed line downstream of the vaporizer. Some sort of high-voltage isolation to electrically isolate a failed thruster is necessary to maintain thruster system reliability and eliminate the need for additional propellant feed systems. For maximum thrusting efficiency the thruster must operate at or near the nodes. The position of the nodes is discussed in Appendix III.

## SECTION IV

## PERFORMANCE TRADEOFFS REALIZED BY POWER SHARING

An analysis was made comparing system weights on synchronous equatorial satellites as a function of battery charge rate, specific impulse of the electric thruster, solar panel specific weight, mission required  $\Delta V$ , mission time, and other secondary factors. Three satellite weights were considered: 2500 lbs, 7000 lbs, and 10,000 lbs\*, with mission lifetimes extending out to a maximum of ten years. Three  $\Delta V$  values were considered: 157, 300, and 635 ft/sec/yr for an impulsive thruster. Figure 12 shows the Isp values selected for the ion engine, based on the available power. This is a function of battery charge rate, mission-required  $\Delta V$ /yr, and % solar panel degradation with time. The satellite power and propulsion system weights increased almost linearly with satellite sizes from 2500 to 10,000 lbs and tradeoffs are similar and relatively independent of satellite size in this weight range. As satellite weight becomes less (<1000 lbs) and thruster station keeping requires less accuracy for satellite positioning, then thruster system "fixed" weights assume more importance.

A digital computer program was developed for this analysis and is presented in Appendix IV. It may be used to compute satellite system weights by putting in selected values of battery charge rate, mission time,  $\Delta V$  energy requirements, etc. PCCS weights for each thruster have been based on the highest power demand for the electric thruster; i.e., for the high-thrust station acquisition or repositioning maneuvers.

Figure 13 shows the calculated thruster system weights based on the data presented in Table I for full power sharing modes, partial power sharing modes, and non-power sharing modes of operation\*\*. The results are shown

---

\* Reference #8 indicates possible economic trends towards large boosters for lifting multithousand pound satellites into synchronous orbits.

\*\*"Full power sharing" is defined as the mode of operation where the thruster uses only that power which is available through sharing the power on a duty cycle with the battery. The thruster may or may not have the available power to operate at its maximum Isp capability. "Partial power sharing" is defined

for a ten-year mission, 10,000 lb synchronous equatorial satellite and a 10 kw load power demand. Battery charge rates of C/4 and C/10 were used with solar panel specific weights of  $\alpha_{sp} = 50$  and 100 lbs/kw. Weights for the full power sharing mode of operation include N/S propellant and tankage weights, propellant and tankage weights for an injection error or initial station acquisition maneuver, two repositioning maneuvers (see Table I), power conditioning and control weights, and thruster engine weights.

For comparison between power sharing and non-power sharing modes of operation, an extra solar panel was provided on the satellite for thruster systems which did not power share, or which required part of their power demands to be supplied with extra solar panels. This extra panel weight was included as a penalty to the thruster system weight. Thus, thruster system weights for a non-power sharing C/20 system and a C/4 system without power sharing would be the same, but each system would have to add about 470 lbs (at  $\alpha_{sp} = 100$  lbs/kw) to provide power to the ion engine to operate at the same Isp as the C/4-ion engine (8500 sec) with power sharing. For the C/10 partial power-sharing mode, an additional panel weight of 286 lbs must be added to increase the ion Isp capability from an average of 2670 secs to 8500 secs (maximum capability).

Table II shows the power budget breakdown for a 10-year, 10,000-lb satellite as a function of battery charge rates of C/4, C/10, and C/20-load power demand is 10 kw. Payload weight is defined as

$$\begin{aligned} \text{Payload weight} = & \text{satellite weight} - \text{thruster system weight} - \\ & \text{structure weight} - \text{solar panel weight} - \text{secondary battery weight.} \end{aligned} \quad (2)$$

As seen, the payload weight will vary depending on the solar panel specific weight and the battery capacity in watt-hrs/lb. As shown in Appendix I, secondary battery reliability increases with increase in charge rate (See Figures 27-30). Therefore, to compare the payload weights for systems that have

---

as the mode of operation where the thruster shares all the power available to it, but requires additional solar panels to bring its Isp capability up to maximum. "Non-power sharing" is defined as that mode of operation where the thruster does not share power, and must penalize the thruster system by adding additional panel weight to bring the Isp capability up to maximum.

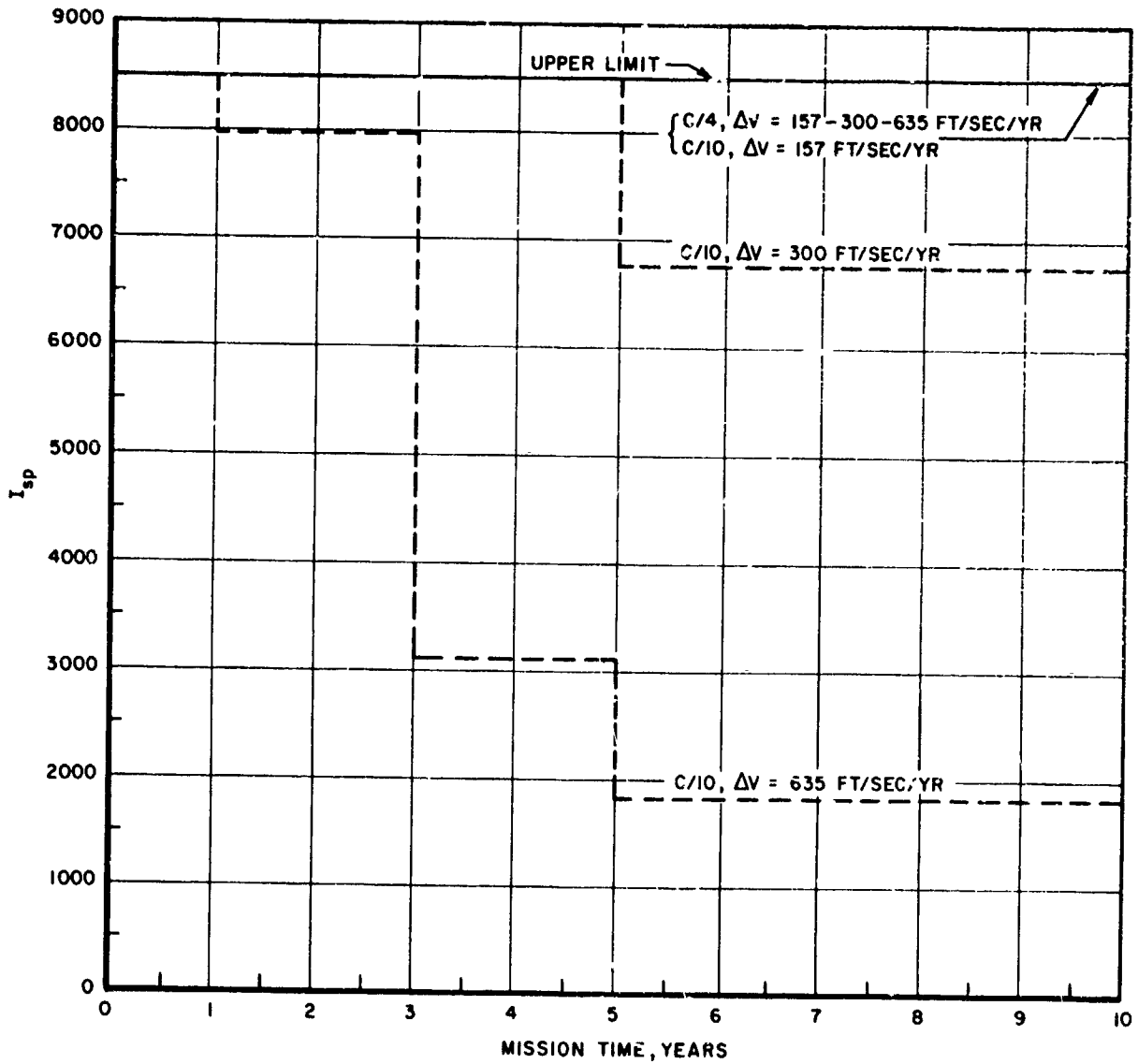


Figure 12.  $I_{sp}$  Values Selected for the Ion Engine Systems

TABLE I

SYNCHRONOUS EQUATORIAL SATELLITE  
PERFORMANCE CHARACTERISTICS

Satellite weight, lbs	2500-7000-10,000
Load power (continuous), kw	2.5-7-10 [1 watt/lb of satellite]
Satellite structural weight, lbs	750-2100-3000
<hr/>	
Mission time, yrs	10
Mission required $\Delta V$ (ft/sec-yr)	157-300-635
Solar power specific weight, $\alpha$ sp, lbs/kw	50-100
Solar panel PCCS efficiency, %	95
10 yr solar panel degradation, %	25
Battery D.O.D., %	70
Battery % overcharge	125-130
Battery charge rate	C/4-C/10
Battery capacity, watt-hrs/lb	8 @ C/4, 10 yrs
Colloid thruster Isp, secs	1500-2000
Ion thruster Isp range, secs	1820-8500*
PCCS weights, ion, lbs/kw	10 @ 5000 secs; 15 @ 8500 secs
PCCS weights, colloid, lbs/kw	10 @ 1500-2000 secs
Ion thruster system efficiency, %	40 @ 1800 secs to 75 @ 8500 secs (See Figure 14)
Colloid thruster system efficiency, %	70 from 1500-2000 secs
Ion thruster specific weight, lbs/kw	2.5 @ 5000 secs; 4 @ 8500 secs
Colloid thruster specific weight, lbs/kw	8 @ 1500-2000 secs
Propellant tankage factor, ion and colloid, %	7% of propellant weight
Required thrust range, N/S station- keeping, ion @ 50% thruster duty cycle	0.85 mlbs @ $\Delta V=157$ ft/sec/yr, 2500 lbs satellite; to 13.8 mlbs @ $\Delta V=635$ ft/sec/yr, 10,000 lbs satellite

TABLE I (Cont'd)

Required thrust range, N/S station keeping colloid @ 25% thruster duty cycle	1.57 mlbs @ $\Delta V=157$ ft/sec/yr, 2500 lbs satellite; to 24.1 mlbs @ $\Delta V=635$ ft/sec/yr, 10,000 lbs satellite
Required thrust level for injection error removal, initial station acquisition ( $\Delta V=125$ ft/sec), & repositioning at $5^\circ$ /day (two maneuvers, $\Delta V=187$ ft/sec)	10 mlbs for 2500 lbs satellite (See Reference 9)
Ion Isp for injection error removal, initial station acquisition, repositioning	5000 secs**
Colloid Isp for injection error removal initial station acquisition, repositioning	1500 secs

\* Accomplished with two different thruster designs; 1820-5000, and 5000-9500 (upper limit). This full range requirements occur only for ion engine operating on the full power sharing mode at charge rate of C/10 and  $\Delta V=635$  ft/sec/yr.

\*\* It is assumed in the analysis that the solar array can be unfurled upon insertion into orbit, whereupon the electric thruster can perform injection error removal and initial station acquisition at high thrust, high power levels prior to the demand by the satellite for full power. The acceleration imparted to the vehicle by the electric thruster during these maneuvers is on the order of  $0.4 \times 10^{-5}$  "g's" and can easily be withstood by flexible roll-up solar arrays (Reference #10). The specific impulse selected for the ion and colloid engines are nominal. Lower selected Isp would increase the required propellant to perform these maneuvers but the required power should be lower; however the PCCS system would be somewhat lighter.

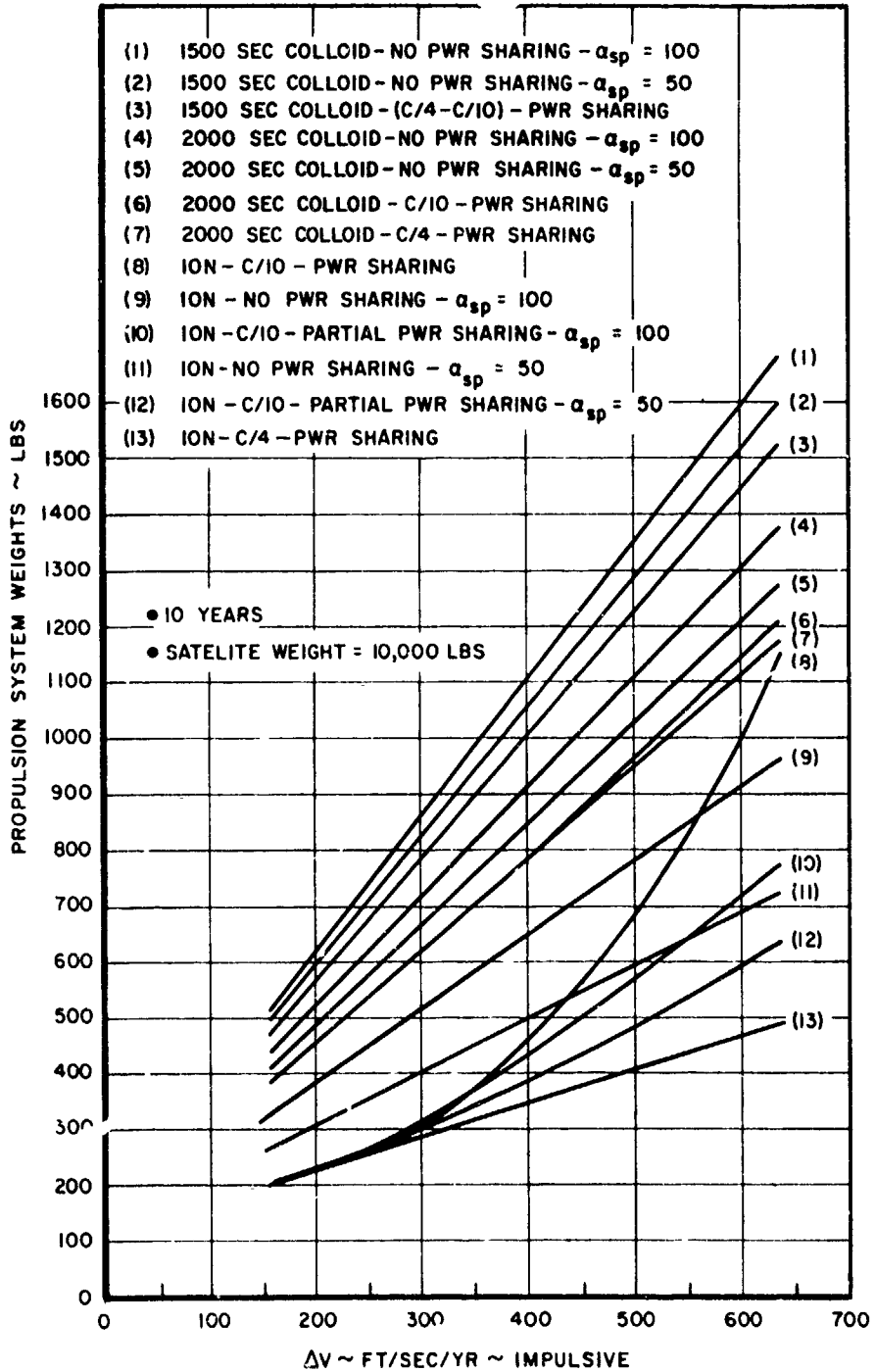


Figure 13. Calculated Weights for Different Thruster Systems

TABLE II  
 SATELLITE POWER BUDGET FOR N/S STATION KEEPING  
 SATELLITE WEIGHT = 10,000 LBS  
 LOAD POWER = 10 KW  
 10 YRS

SELECTED BATTERY CHARGE RATE	BATTERY CHARGE TIME (hrs)	BATTERY CHARGE POWER (kw)	TRICKLE CHARGE POWER (kw)	ARRAY SIZED TO CHG. BATTERY (kw)	ARRAY SIZED FOR EOL (kw)*	ARRAY POWER FOR THRUSTER (kw)	(50% Thruster Duty Cycle)		
							ISP CAPABILITY (SEGS)	ΔV = 157 FT/SEC/YR (IMPULSIVE)	ΔV = 300 FT/SEC/YR (IMPULSIVE)
C/20	18.9	0.86	.343 C/50	10.860	15.2	***	-----	-----	-----
C/10	9.1	1.71	.343 C/50	11.71	16.4	6.06 KW BOL to 1.37 KW	8500**	8500** BOL to 6753 EOL (7550 avg)	8500** BOL to 1823 EOL (2670 avg)
C/4	3.4	4.28	.428 C/40	14.28	20.0	9.57 KW BOL to 3.85 KW EOL	8500**	8500**	8500**

\* Includes 5% PCCS losses.  
 \*\* Ion thruster upper limit.  
 \*\*\* During the eclipse periods of the satellite, (two 45-day periods) only the excess solar array power (that array added for EOL degradation) is available to a thruster (BOL) for the required duty cycle of the ion engine (12 hours per orbit). This power decreases rapidly with time and is essentially only a small fraction of the power required by the ion engine after five years. During the non-eclipse season (the remaining 75% of the year), the full power of 4.86 kw would be available at BOL (battery charge power - trickle charge power + excess array power due to EOL sizing) but would decrease to about .514 kw after five years. Station keeping could be performed at high Isp during part of the non-eclipse mission, but after five years at ΔV = 157 ft/sec/yr no station keeping could be performed efficiently during the eclipse season. This would probably not be acceptable to spacecraft designers and certainly would not be practical at ΔV's much in excess of 157 ft/sec/yr.

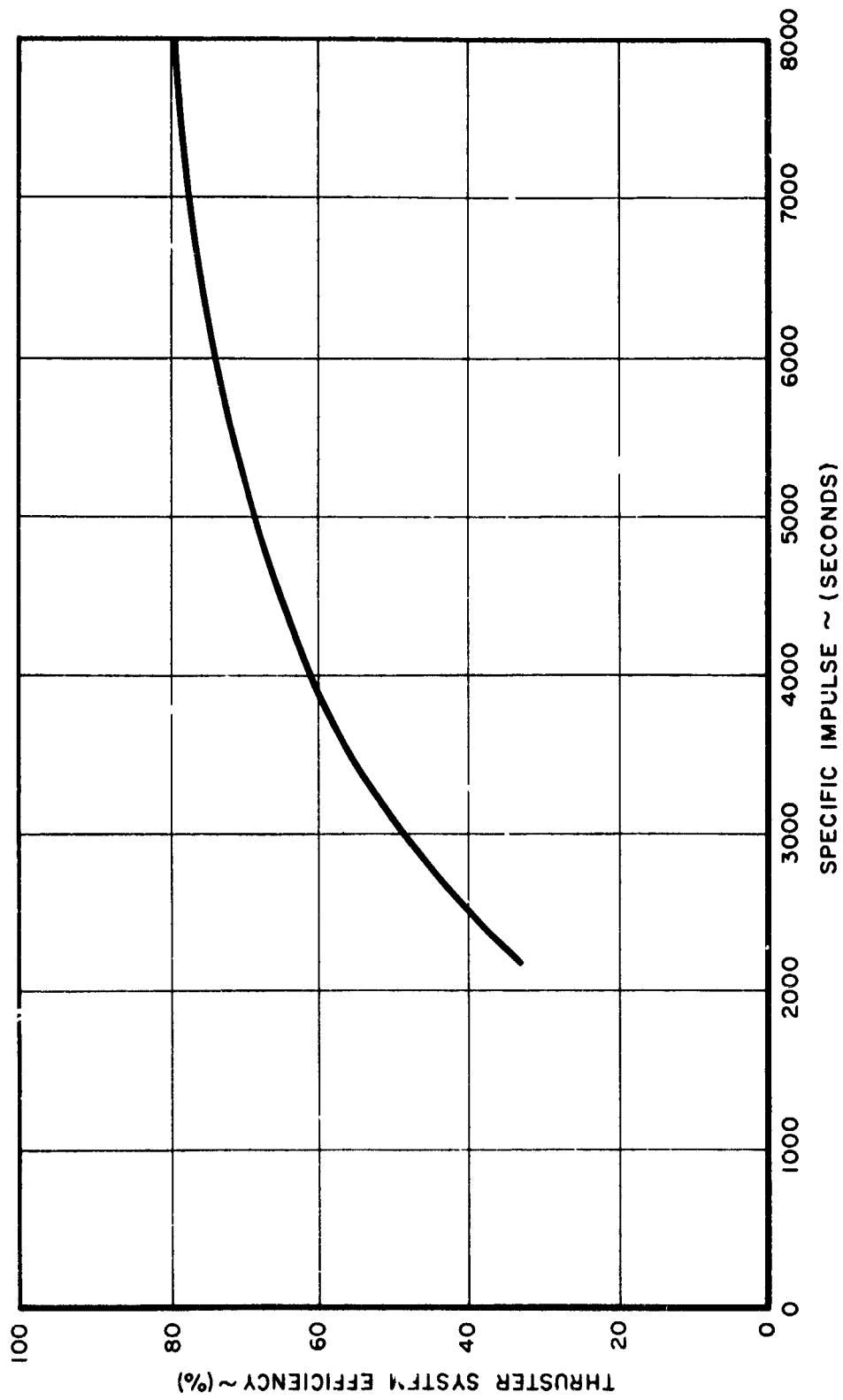


Figure 14. System Performance for Bombardment Ion Engine of Millipound Thrust Size

different battery charge rates, we need to have some idea of secondary battery weights as a function of charge rate, so that the battery system may be sized to maintain reliability. Battery weight for the C/4 charge rate was based on the ten year baseline capacity of 8 watt-hrs/lb. When the battery charge rate is selected on the basis of the tradeoffs between increased battery reliability at higher charge rate and increased solar panel sizing for this higher charge rate, then the reliability at C/10 and  $\alpha_{sp} = 100$  lbs/kw must be about 4.6% better than at C/20. In turn, battery reliability must be at least 14.4% better at C/4 than C/10 if the combined solar panel and C/4 battery weights are to be no more than the C/10 weights. Figures 15 and 16 illustrate this.

For the comparative analysis, we assumed that battery reliability as a function of battery charge rate will be at least as high as that shown in Figures 15 and 16. Therefore, in calculating the payload weight, we assumed the summation of battery and solar panel weights to be constant so that the effect of propulsion system weight on payload capability is clearly shown. If battery reliability is greater than that shown, then payload improvement from optimizing thruster performance will be even greater.

Figure 17 shows the payload improvement realized by using ion thruster systems operating in various degrees of power sharing versus non-power-sharing ion engine. Figures 18 and 19 show the payload improvement realized by using ion engines operating in various degrees of power sharing compared to 1500 and 2000 sec colloid engines with power sharing. The payload improvement shown in Figures 17-19 is relatively independent of satellite size, at least in the 2500-10,000 lb satellite size range considered.

The influence of mission time on percent payload increase through power sharing is indicated in Figures 20 and 21 for two satellite total impulse extremes based on 157 and 635 ft/sec/yr and satellite weights of 2500 lbs and 10,000 lbs, respectively. This indicates that decreasing mission time tends to reduce the advantage of power sharing. Note that the amount of mission time when the ion engine has 0% or less system weight advantage over the colloid engine is very short. This time is a function of the initial propulsion system weights including thruster weight, and orbit-injection error-correction and initial

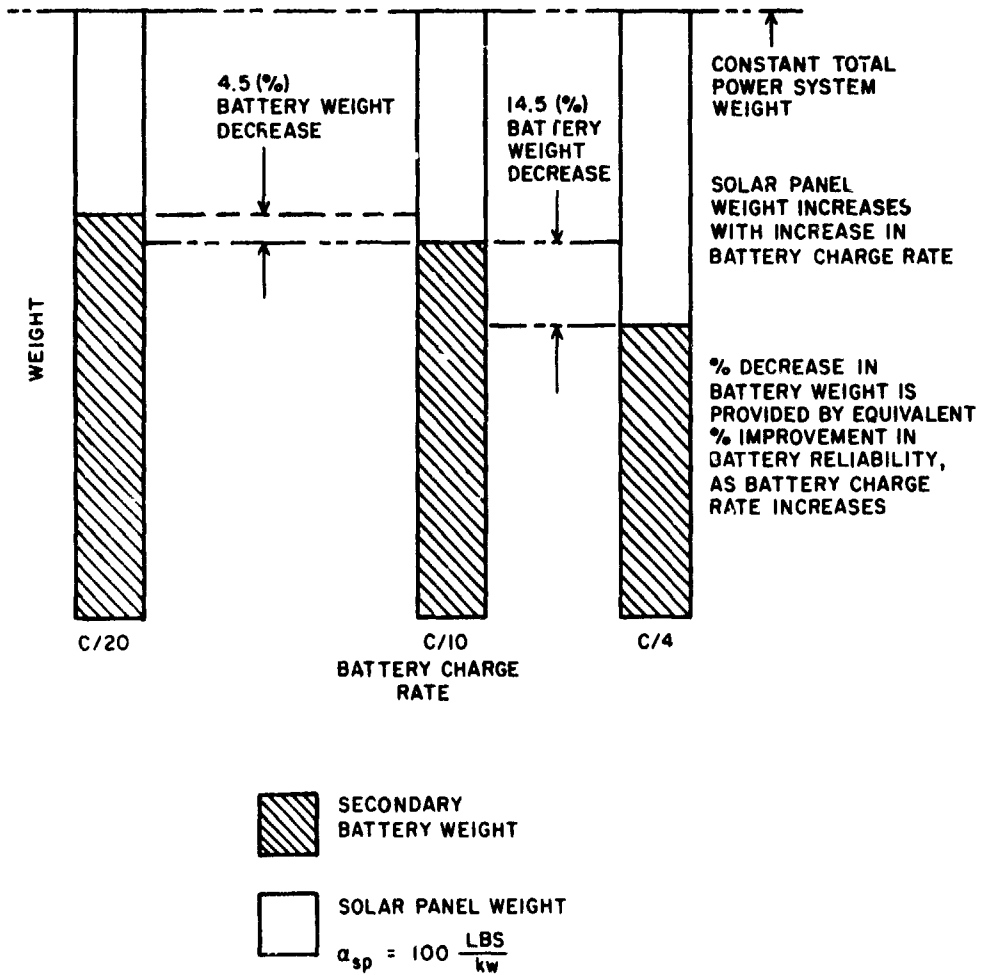


Figure 15. Secondary Battery/Solar Panel System Weight Tradeoffs as a Function of Battery Charge Rate, With Solar Panel  $\alpha_{sp} = 100 \text{ lbs/kw}$

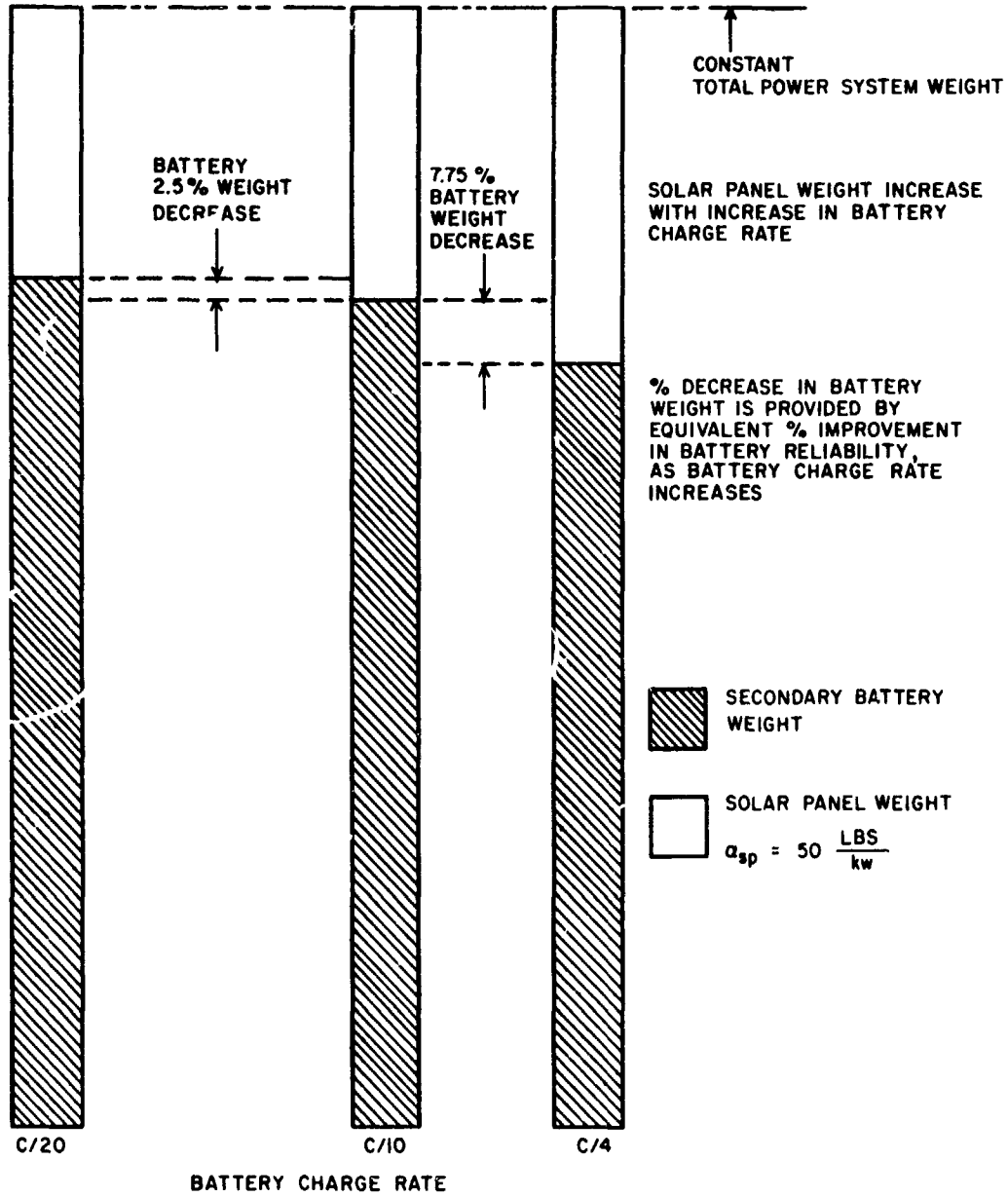


Figure 16. Secondary Battery/Solar Panel System Weight Tradeoffs as a Function of Battery Charge Rate, With Solar Panel  $\alpha_{sp} = 50 \text{ lbs/kw}$

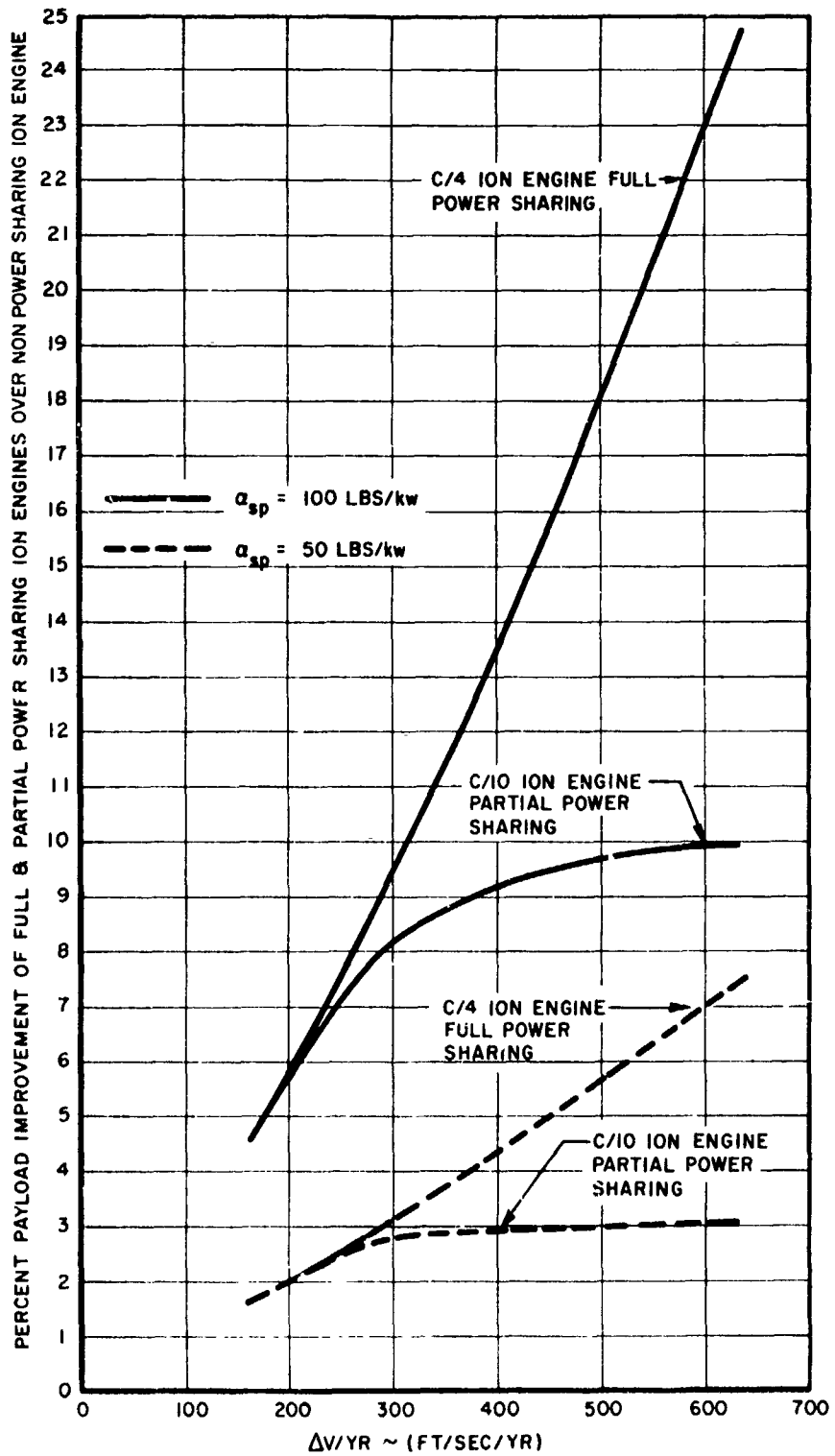


Figure 17. Payload Improvement of Ion Thrusters Using Full and Partial Power Sharing, Versus Non-Power-Sharing Ion Engine

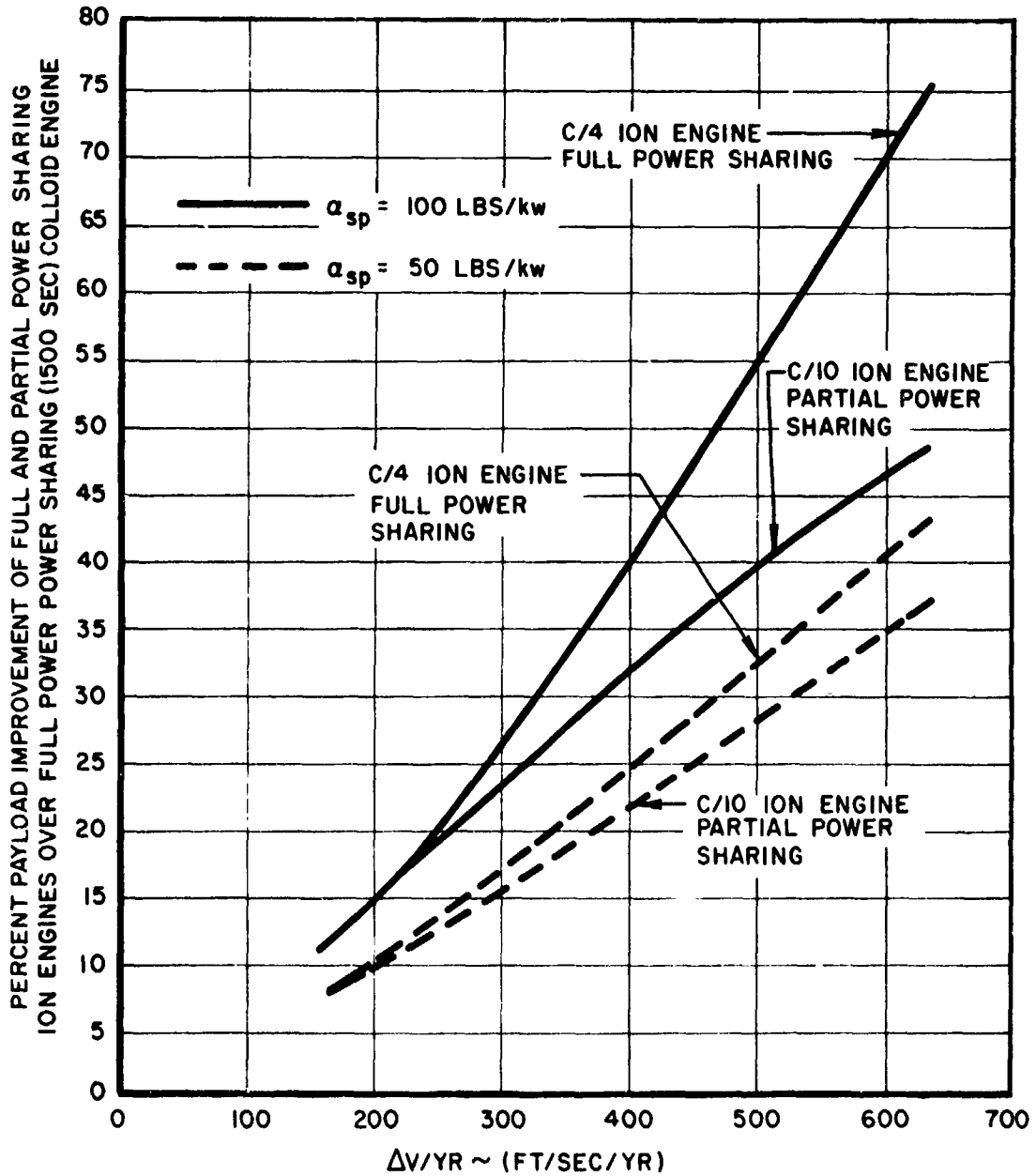


Figure 18. Payload Improvement of Ion Thruster Using Full and Partial Power Sharing, vs 1500 Sec Colloid Thruster Using Full Power Sharing

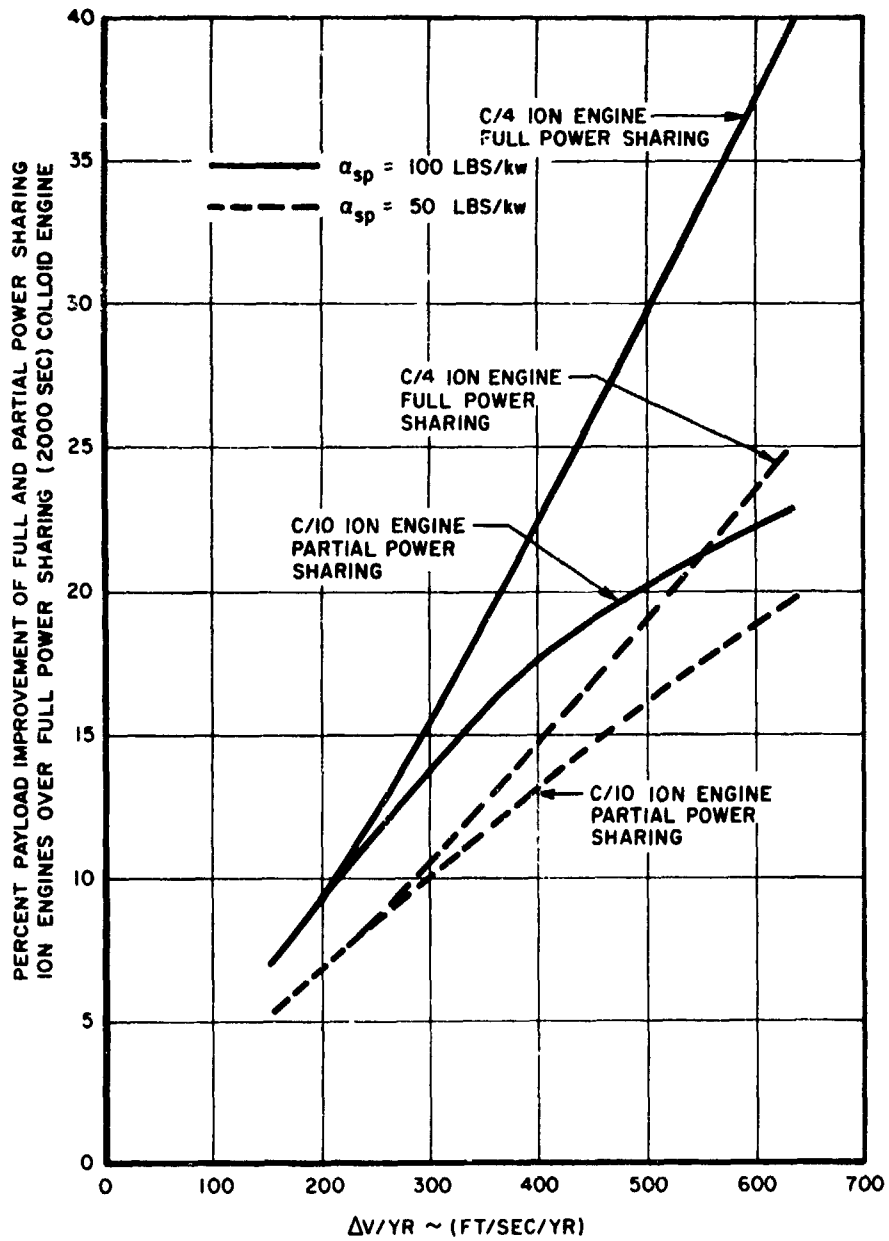


Figure 19. Payload Improvement of Ion Thruster Using Full and Partial Power Sharing, vs 2000 Sec Colloid Thruster Using Full Power Sharing

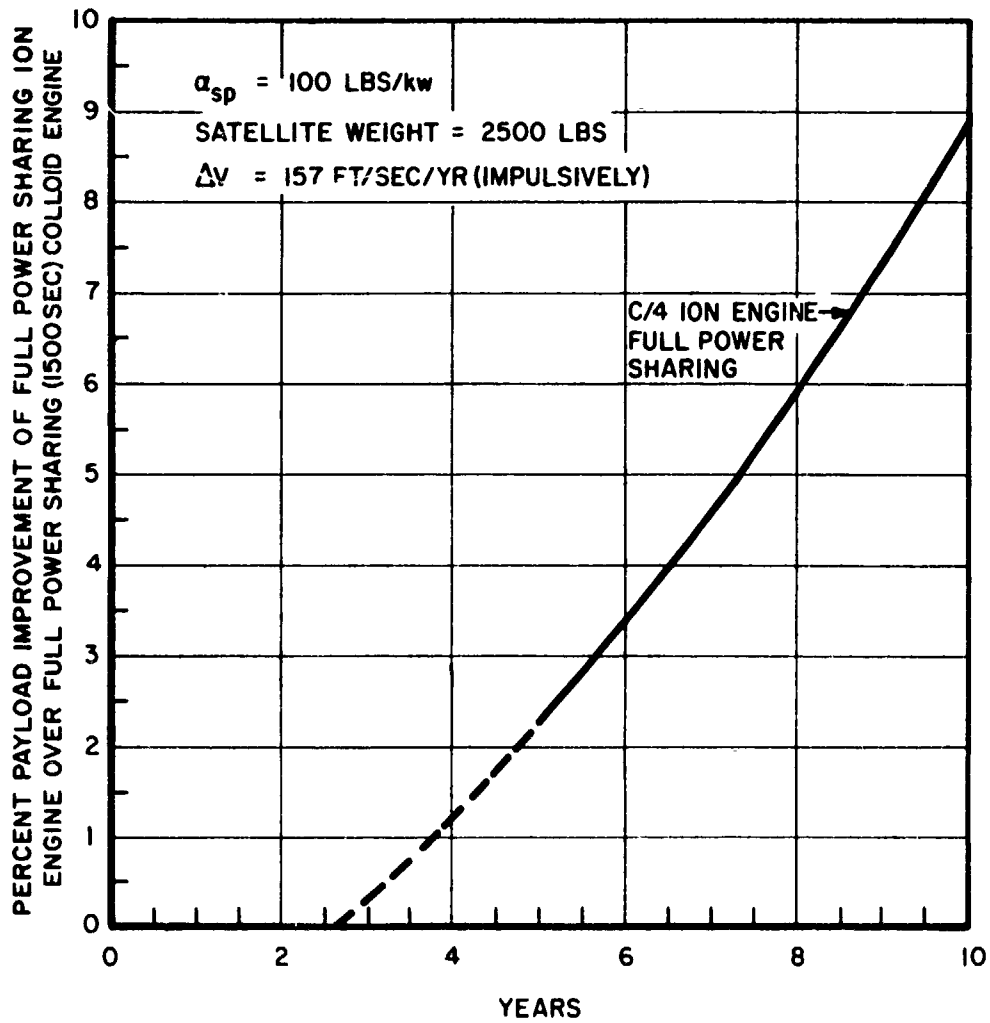


Figure 20. Payload Improvement Realized With Power Sharing as a Function of Mission Time

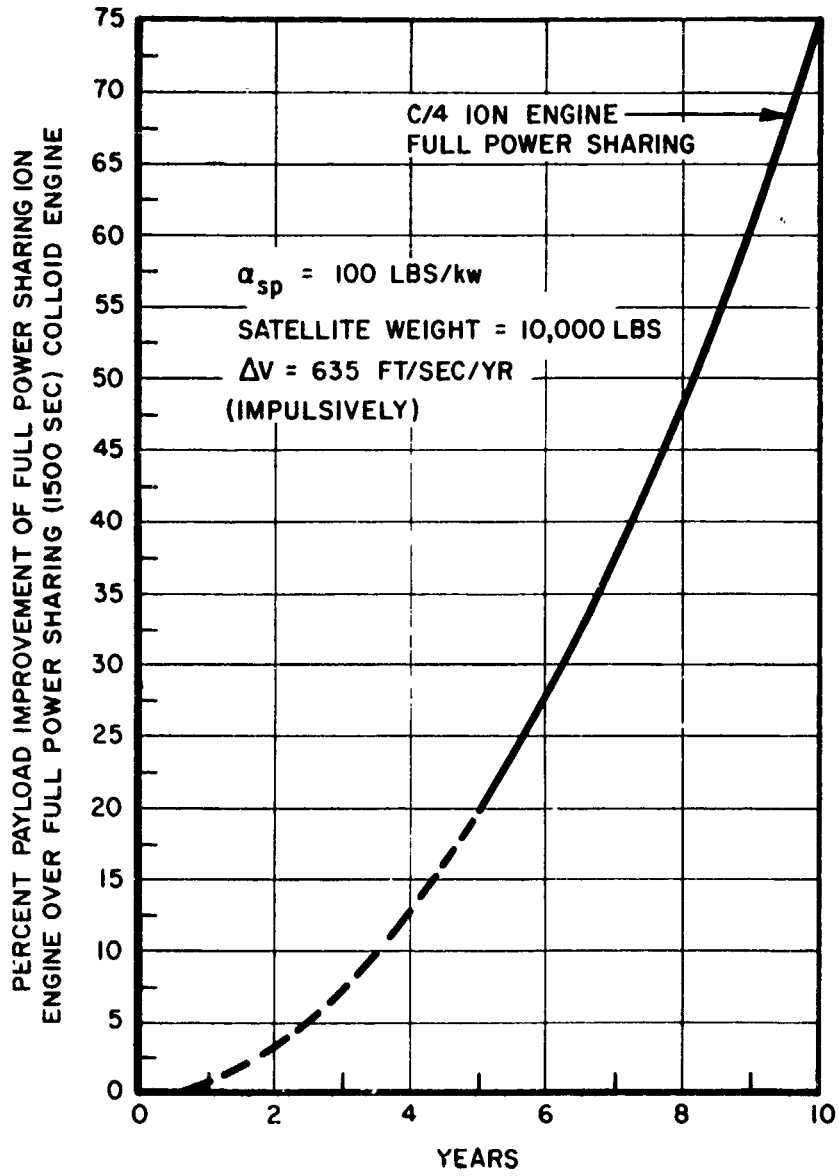


Figure 21. Payload Improvement Realized With Power Sharing as a Function of Mission Time

AFAPL-TR-71-42

station acquisition propulsion system weights. If these weights are the same for the ion and the colloid system, then the cross-over time is at zero years, and the power-sharing ion engine always provides a payload improvement.

SECTION V

CONCLUSIONS AND RECOMMENDATIONS

1. Battery capacity and reliability factors, influenced by high D. O. D. (70%) and long mission times (up to ten years), may dictate a battery charge rate in the neighborhood of  $C/10$  to  $C/4$  [increased solar array weight traded off with increased battery reliability (or reduced battery weight)] (See Figures 27-30).
2. Electric propulsion may take advantage of the need for a high battery charge rate and thus minimize propulsion system weights for mission functions such as N/S station keeping and elimination of rotation of line of apsides.
  - a. Optimization of ion engine Isp in the multithousand pound satellite class with load power demands in the neighborhood of 1 watt/lb of satellite weight, can increase useful payload capability from a few percent up to 25% compared to a non-power sharing ion engine; and from 50 to 75% compared to a power-sharing colloid engine operating between 1500-2000 sec (see Figures 17-19).
  - b. The  $C/10$  and  $C/4$  charge rates will provide about the same payload improvement up to  $\Delta V = 300$  ft/sec/yr; beyond that point,  $C/4$  improvement is greater.
  - c. Figure 13 shows that with 23 additional pounds (5% more propulsion system weight) for the  $C/4$  battery charging mode, the ion engine can provide over four times the N/S station keeping accuracy provided by the 1500-second colloid engine (635 ft/sec/yr compared to 157 ft/sec/yr).
3. Booster costs can be reduced significantly by launching one large satellite rather than several smaller ones.
4. From a propulsion system weight standpoint, if engines with different Isp values have about the same "fixed" weights, the higher Isp system will have the lowest system weight and provide the maximum payload capability for all mission times (see Figures 20 and 21).
5. A program should be initiated to investigate the influence of secondary battery charge rate on battery system capacity and reliability for 24-synchronous

**AFAPL-TR-71-42**

**orbits. Depth-of-discharge and temperature should be held constant while charge rate is varied; cycle life should be determined for these systems at the kw-load power level.**

**6. Work should be done on multi-kilowatt size ion engines with performance capability of constant thrust, variable Isp of 5000-8500 seconds and 1800-5000 seconds (two different systems). Ground-based long-term tests should be planned.**

**7. A feed system isolator should be developed to provide the capability, at least, of electrically isolating a thruster from a common feed system in the event of a high voltage failure of the thruster system.**

APPENDIX I  
BATTERY ANALYSIS

1. SELECTION OF SECONDARY BATTERY OPERATING CONDITIONS

a. Depth of Discharge (D.O.D.)

During the eclipse portion of any orbit, the secondary battery supplies the electrical power to the spacecraft. To minimize the battery weight for a synchronous orbit, the D.O.D. for the battery should be at least 50%, and preferably 70-80%. The effect of D.O.D. on battery weight is shown in Figure 22 (Reference 3, page 141). Tests by the Inland Testing Laboratories, the Quality Evaluation Laboratory, and others, however, indicate that cell cycle life decreases with increasing D.O.D. (Reference 11).

b. Allowable Charge Rate and Temperature

Most of the literature available on batteries is for charge-discharge cycles in near-earth orbits, where charge rates must necessarily be high because charge time is so short (55 minutes). In near-earth orbits, the D.O.D. is necessarily low because the deeper the D.O.D. the higher the charge rate (and charging power) required to fully recharge the battery. Also, near-earth orbits require a lower D.O.D. because cell reliability decreases with increased DOD; a near-earth orbit requires about 16 times as many charge-discharge cycles per day as a 24-hour orbit.

It is difficult to separate the factors that determine optimum battery charge rate. As already stated, there is little data available for synchronous-orbit type conditions. In most tests, one or more important variables is changed from test to test. For example, charging rate may be held constant, but both DOD and temperature may be varied. This makes it difficult to determine which parameter most influenced the data. However, data is available that shows the general relationship of temperature and charge rate to the so-called cell "critical voltage" (the voltage when either the internal pressure or temperature, or both, increase to a point that can adversely affect cell life and reliability). Critical voltage is not well defined, but it occurs during cell overcharge conditions.\*

\*Overcharge: the condition where, because of charging inefficiencies, the battery must accept electrical energy in excess of its nominal electrochemical

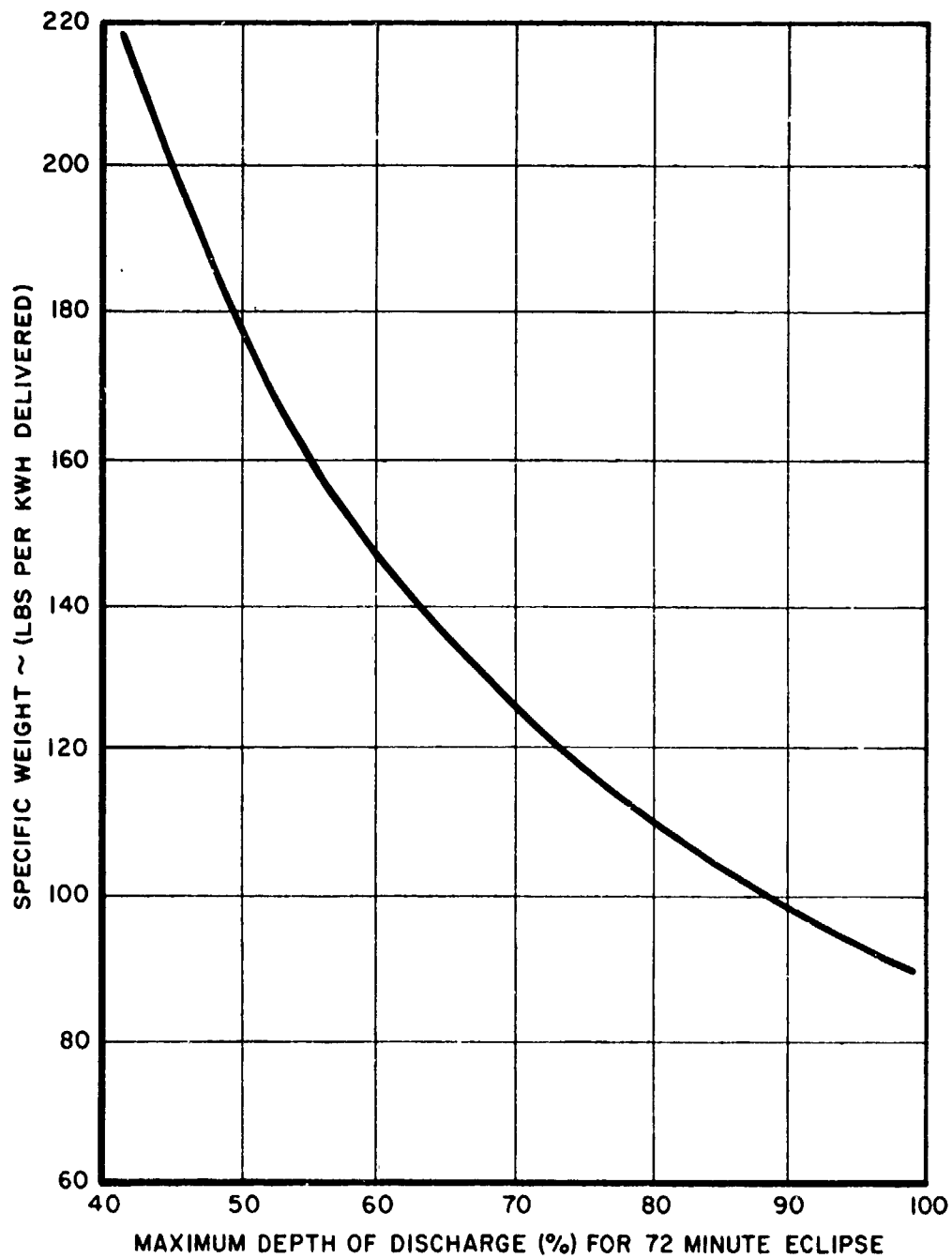


Figure 22. Influence of Depth of Discharge on Battery Specific Weight

Figure 23 shows this relationship (References 3, page 35; 11, page 85; and 12, page 410).

c. Influence of Temperature and Charge Rate on Cell Capacity and Efficiency

The fact that the critical or terminal cell voltage is higher for higher charge rates and lower temperatures indicates that battery charging efficiency is higher under these conditions. Capacity decreases by 10-20% in going from 50 to 100°F for voltage limits in Figure 23, and this decrease is larger at low charge currents. Higher charge rates can cause hydrogen evolution at low temperatures, however, so one must be careful when optimizing charge acceptance over the entire temperature range to also adjust charge rate and voltage limit as a function of cell temperature (Reference 3, page 37). Figure 24 shows the influence of temperature on available cell capacity (Reference 11, page 87).

The % overcharge required to fully recharge a battery is termed an efficiency loss because a 120% overcharge requires that 120 AH be put in to bring a 100 AH battery back to full capacity. This efficiency loss is of no significance to the solar panels, but it does affect the heat output from the battery during recharging and the length of time required to recharge. Figure 25 shows cell voltage as a function of cell temperature and battery charge rate during overcharge (Reference 11, page 87). Cell voltage in the overcharge condition is lower if cell temperature is high and charge rate is low.

Figure 26 shows the influence of charge rate and temperature on % overcharge required to recharge, and the allowed overcharge before the maximum tolerable voltage is reached (critical voltage) (Reference 11, page 87). The solid lines, obtained from Figures 4-12, 4-13, 4-14, and 4-15 of Reference 11, indicate the % overcharge required to fully recharge the battery. As charge rate increases, battery charge efficiency increases. The dotted lines show the capability (trend only) of the battery to recharge; this is a function of the critical voltage (Figure 23) and the actual voltage conditions (Figure 25). At 60°F, for

---

capacity in order to bring it back to full capacity. In many instances "full charge" (100%) is defined as the condition when the nominal rated battery ampere hours have been put into the system, although because of efficiency losses the battery has not attained its original available cell capacity.

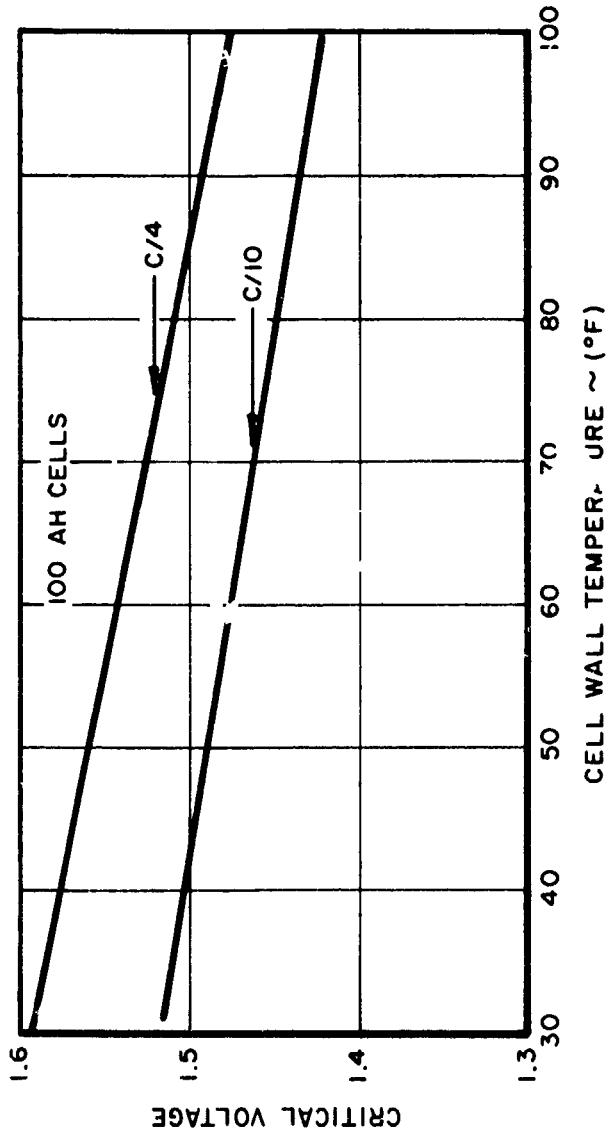


Figure 23. Critical Charge Voltage as a Function of Cell Temperature and Charge Rate

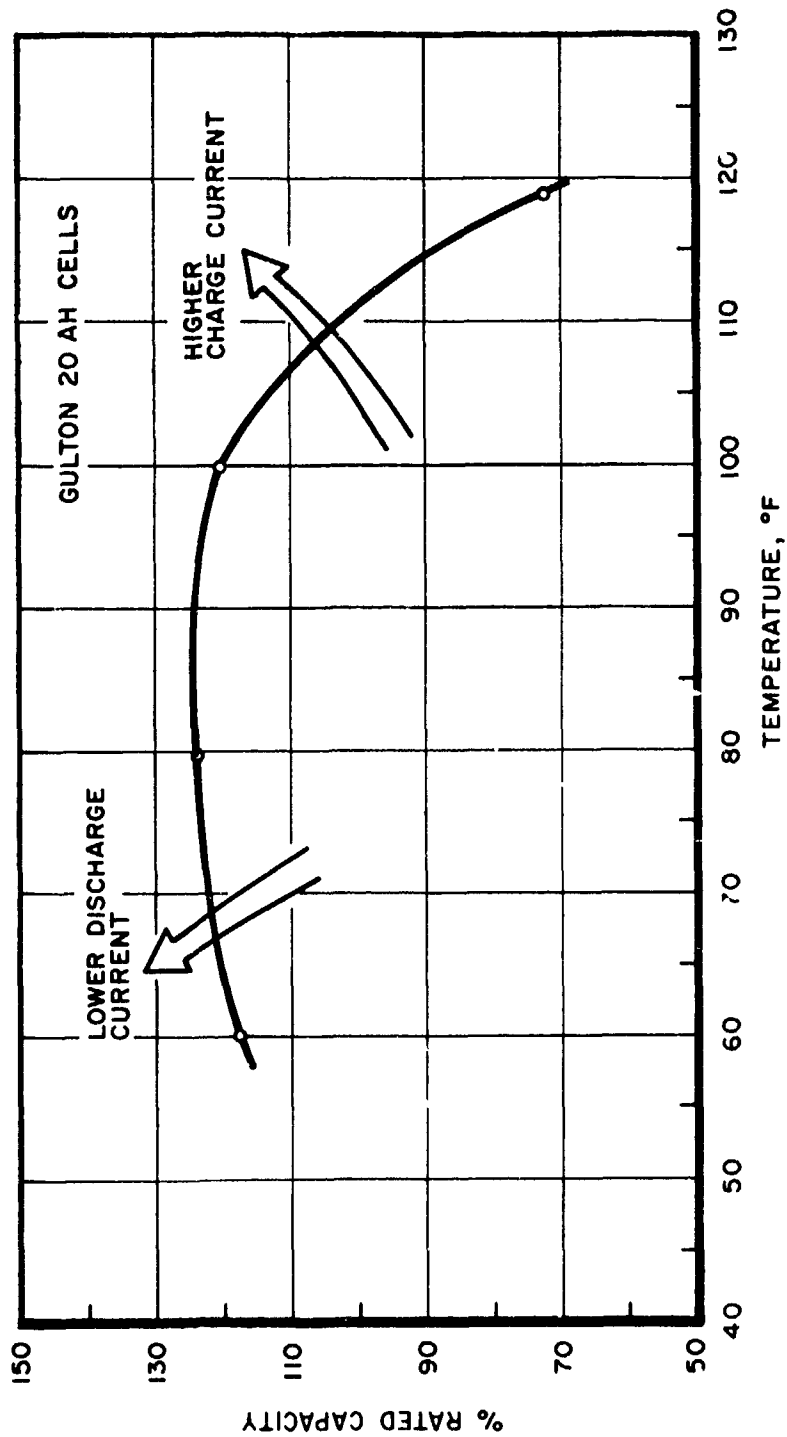


Figure 24. Available Capacity Vs Temperature

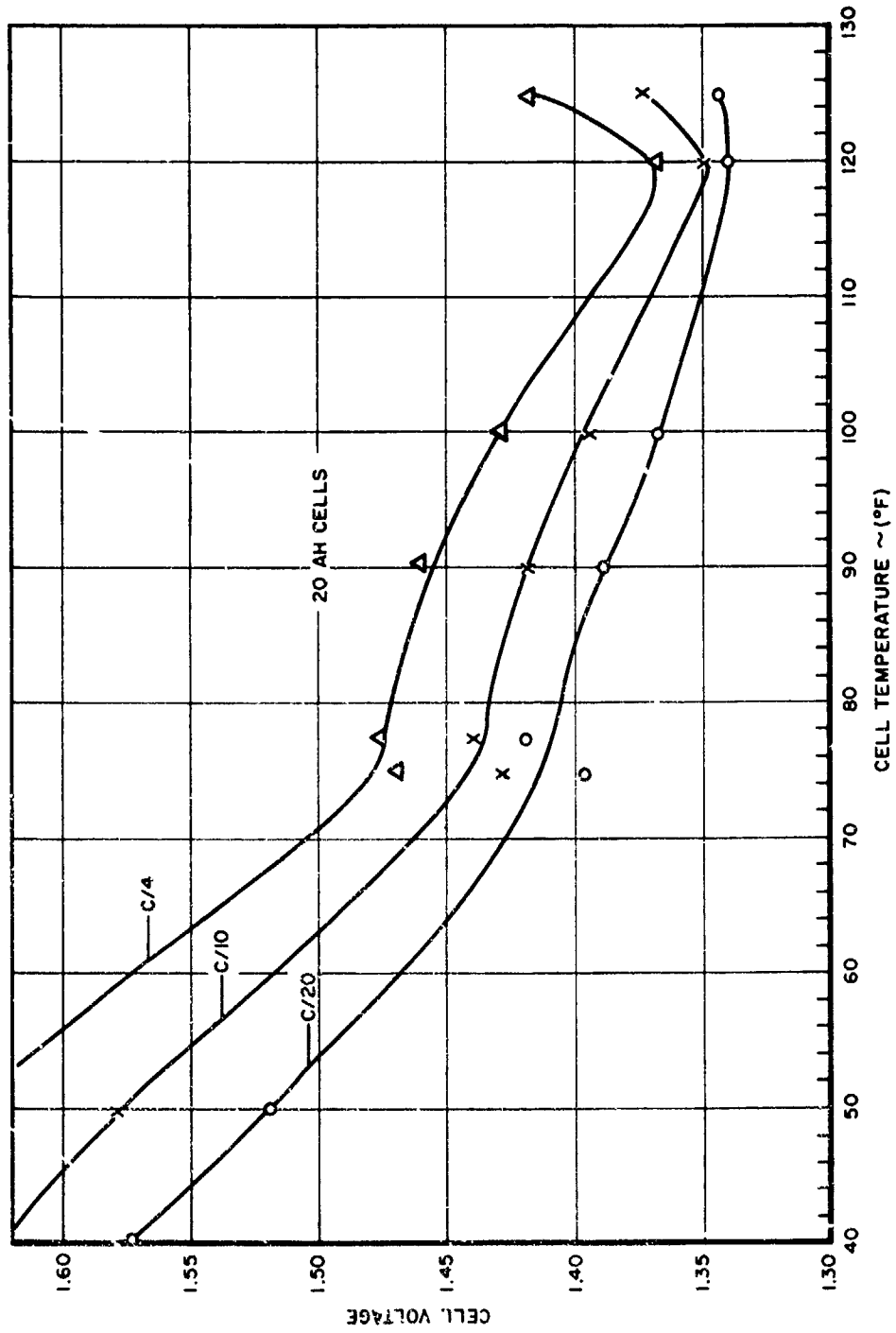


Figure 25. Cell Voltage as a Function of Cell Temperature and Battery Charge Rate

example, the critical voltage at C/10 charge rate, as shown in Figure 23, is 1.475 volts; at this charge rate and battery temperature, the cell voltage would be 1.517 volts as shown in Figure 25. At the stated conditions, therefore, the battery could not be completely recharged. The dotted line in Figure 26 (at C/10 and 60 F) is below the solid line; this shows that to fully recharge the battery at this temperature, we must use either a higher charge rate or a longer charge period. As cell temperature rises the battery can become fully charged at the C/10 rate, up to the temperature where thermal runaway begins; however at this rate the charging efficiency will be lower.

d. Influence of Charge Rate, Temperature, and D.O.D. on Battery Reliability

Figure 27 shows the influence of temperature on cell reliability by indicating the percent of cell groups completing different numbers of life cycles. These cells were operating on a 1.5 to 3-hour cycle (high charge rate) and low depth of discharge (15-20%). It is difficult to extrapolate data from low to high D.O.D. to predict cell reliability for batteries in synchronous orbit, but the data shows a trend toward improved reliability at lower temperature (Reference 11, page 90-92).

Tests by industry laboratories indicate that cell cycle life decreases with increasing D.O.D. (Reference 3, page 35). Figure 28 shows the influence of depth of discharge and charge rate on cell cycle life (Reference 11, page 115, 117). The data is for relatively low D.O.D. and high charge rates (the cycle life is 1.5 to 3 hours), but it indicates that cycle life decreases rapidly with deeper D.O. Assuming that the charge rates for these short cycles are determined by the orbital dark/light time ratios, we can estimate the required charge rates and graph these rates versus cycle life; Figure 29 shows the results for 50°F and two values of depth of discharge. These charge rates are based on a 120% overcharge value, and an average cycle life versus cycle time as determined from Figure 28.

Data in Reference 3, page 145, 160 was cross plotted in Figure 30 to yield cell reliability as a function of charge rate, with temperature and D.O.D. being held constant. First, the cell voltage during eclipse discharge, versus the

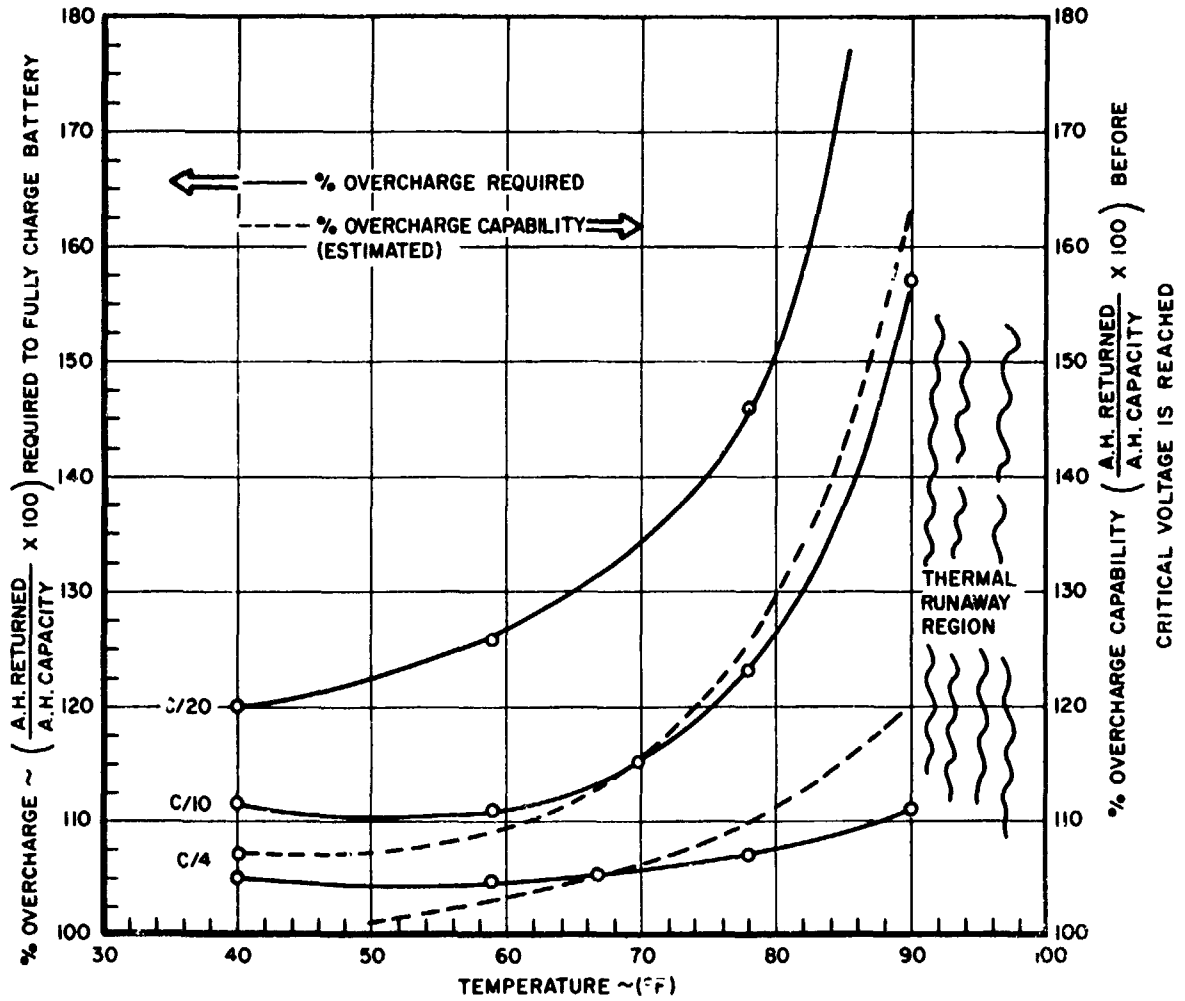


Figure 26. Influence of Charge Rate and Temperature on Recharge Efficiency

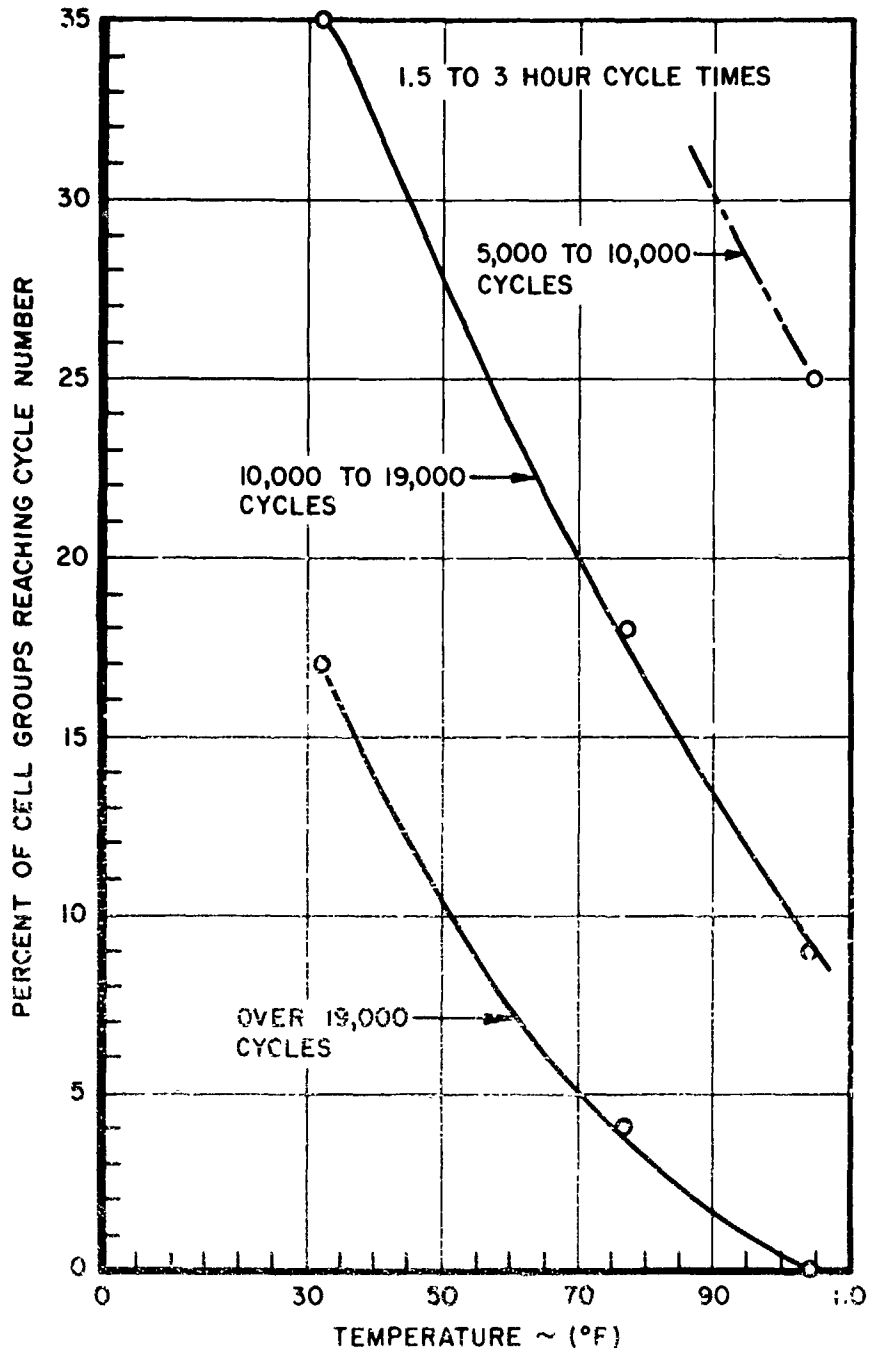


Figure 27. Influence of Battery Temperature on Cycle Life

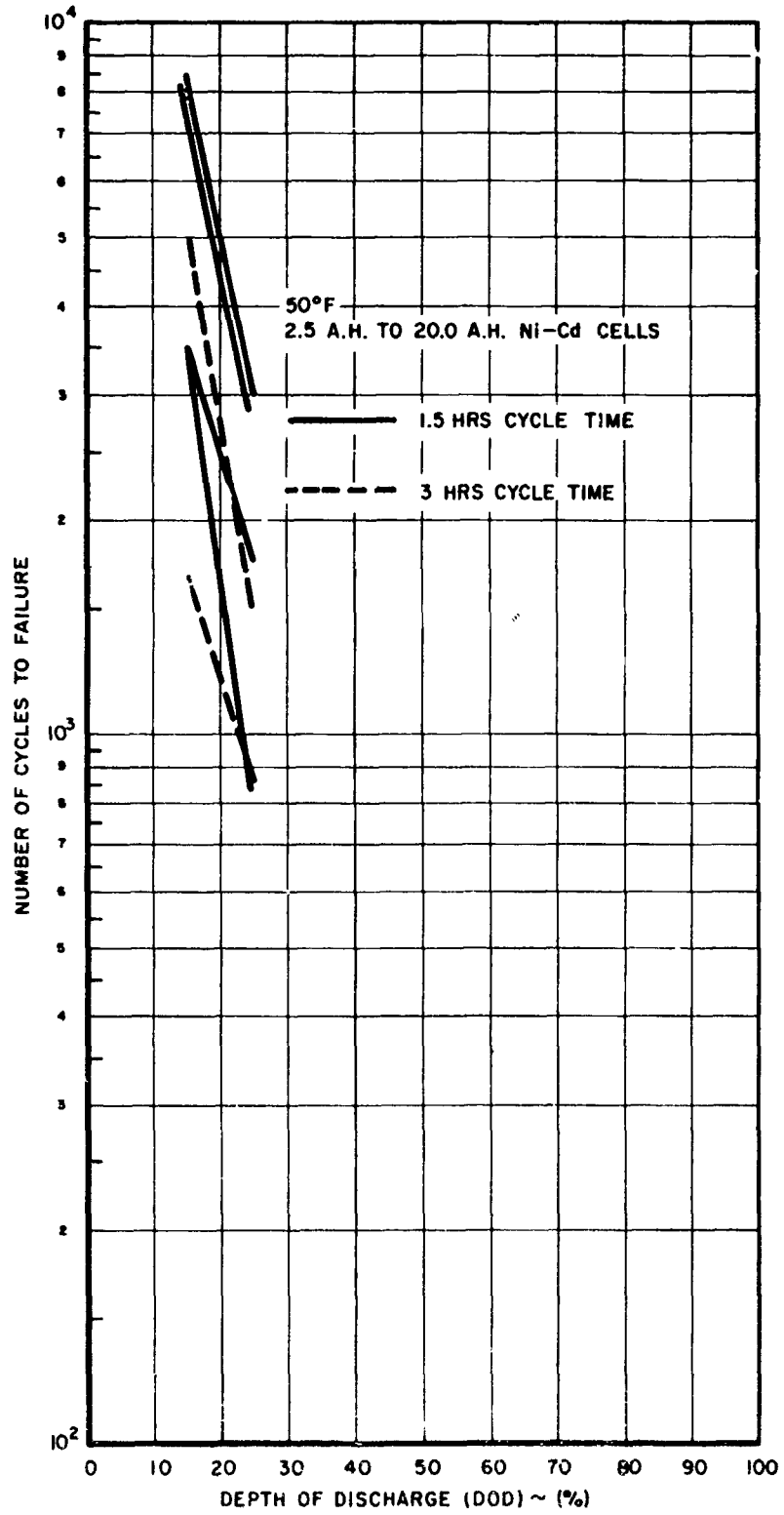


Figure 28. Cycle Life of Ni-Cd Cells

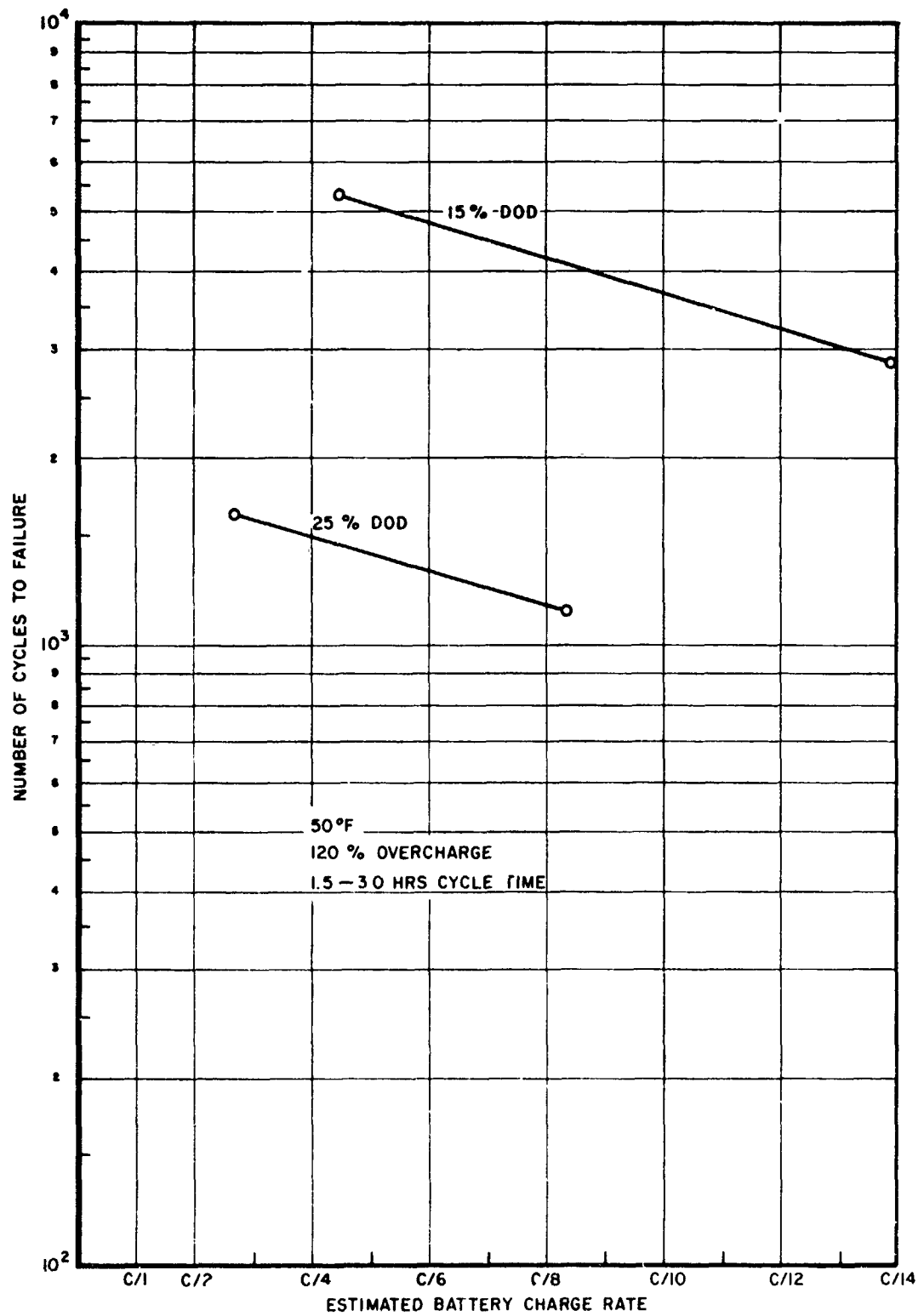


Figure 29. Influence of Charge Rate on Battery Cycle Life

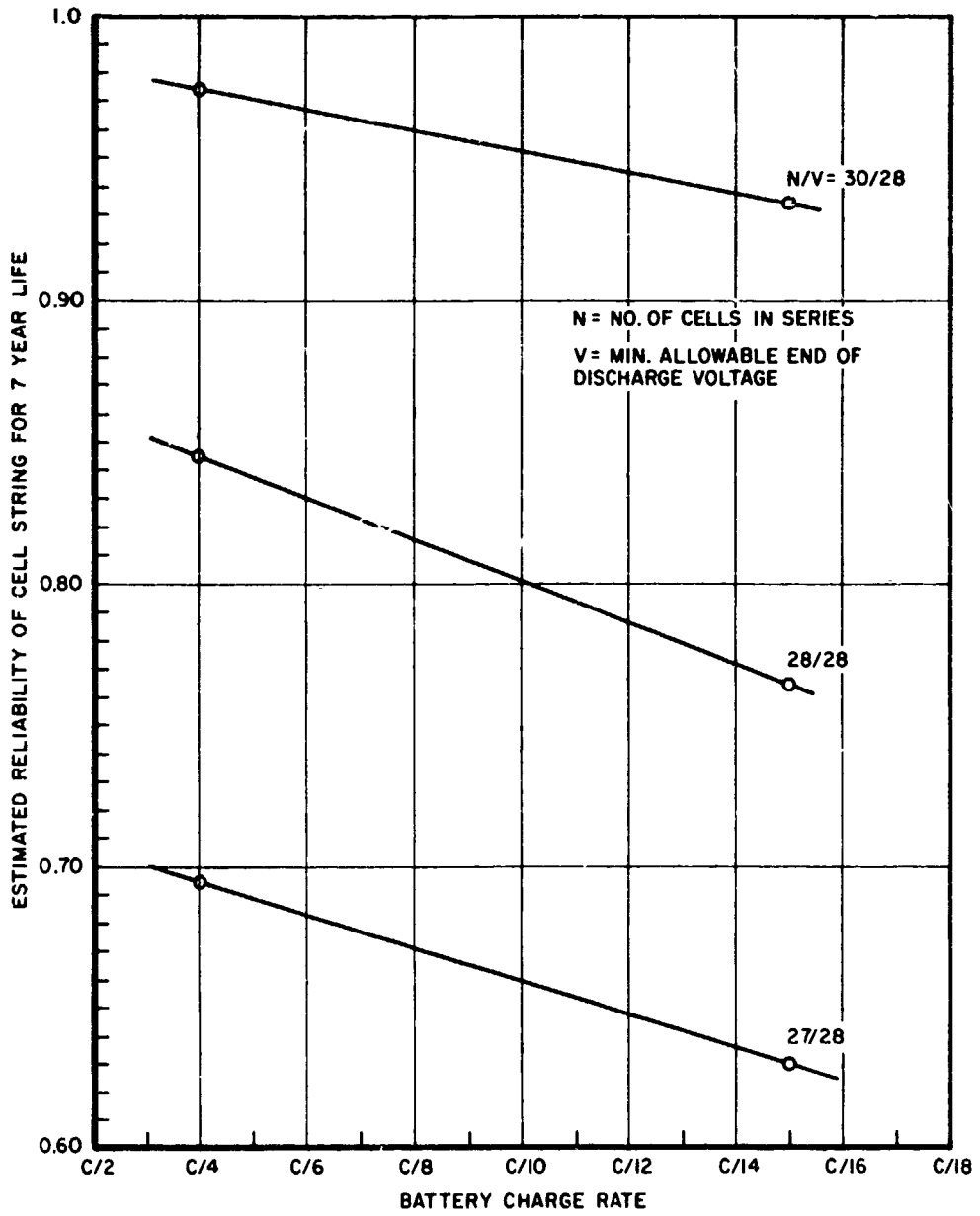


Figure 30. Influence of Battery Charge Rate and Cell Stringing on Cell String Reliability

number of simulated eclipse seasons was determined. Then the predicted reliability of a cell string for a 7-year life versus average end-of-life was determined. A given temperature and D.O.D. for the 14th eclipse season (7-year cycle life) was selected, the voltage read, and the cell reliability for this EOD voltage determined. The results, plotted in Figure 30 show a trend toward higher reliability when charge rate is increased, in this case from C/15 to C/4.

Tests have been performed on cells at synchronous-orbit conditions at the Quality Evaluation Laboratory, Nad Crane, Indiana. Unfortunately, temperature and D.O.D varied from test to test so that the influence of varying charge rates on cycle life could not be determined. Also, most of the tests used the same charge rate, C/30.

e. Some General Theoretical Considerations for Influence of Charge Rate on Battery Performance

Data on the influence of charge rate on the chemical characteristics is limited but indicates the following: high temperature and low charge rate tend to dissolve the cadmium hydroxide in a battery; large cadmium crystals form, which are deposited at the negative (Cd) electrode. This reduces the active surface area of the negative electrode when the charge rate is reduced from C/4 to C/20. On subsequent discharge, this deposit increases polarization\*, which can cause a loss in measured capacity (References 3, page 38; 11, page 77-78, 86). Thus, higher charge rates and lower temperature can maintain high cell capacity provided the low temperature does not prevent the complete recharge of the battery (Figure 24) before the maximum tolerable voltage is reached (Figure 26). If this is the case, charging must continue at some lower level of current to achieve the fully charged state (Reference 11, page 87).

## 2. CHARGE CONTROL

High charge rates and high internal cell temperatures increase the rate of oxygen gas evolution at any state of battery charge. As the battery is being charged, oxygen evolution begins to increase, but this is offset by the increase in oxygen recombination (higher at higher temperature). As the cell voltage

\*A shift in the potential of the battery from the open circuit voltage which results from the flow of current through the battery in either direction.

approaches its desired end-of-charge level, the oxygen evolution rate begins to exceed the recombination rate and the internal pressure begins to rise. Therefore, the higher the temperature, the higher the overcharge current can be without increasing the pressure (Reference 3, page 32) so that higher cell voltage can be permitted (Figure 23). Rapid charging of sealed Ni-Cd cells, however, requires special sensors and controls to prevent excessive overcharging which may result in a dangerous rise in internal pressure. If these sensors and controls are efficient, experimental data indicates "there is no upper limit on the charging rate that a cell will accept at high efficiency without damage, provided that the cell is not subjected to overcharging at the high rates" (Reference 13, page 393). In other words, no damage will result to the cell if overcharge is detected immediately and a somewhat lower rate of charge is used until full capacity is reached. The charge rate selected, then, depends more on the selected design of the spacecraft and on the available charging power from the solar array, than on the technical factors influencing the battery. It is the overcharging period, and not the charging period that could be somewhat hazardous (Reference 3, page 32), so the onset of overcharge must be detected immediately and steps taken to reduce the overcharge current to a safe rate.

#### a. Possible Charge Control Methods

(1) Battery Current Limit Methods. The charge current may be limited to that level which can be tolerated under the worst overcharge conditions. A single constant charge level is limited to  $C/20$  in the 30-40°F temperature range, however, because, at a charge rate higher than this, excessive oxygen pressure is generated during overcharge (Reference 3, page 58). An improvement on this technique would be to sense some parameter, such as cell gas pressure, which begins to increase during overcharge, and limit charging to a lower current level. Current limit control schemes are shown in Figure 31.

(2) Battery Voltage Limit Methods. Charging may be limited by establishing a fixed upper level of charging voltage. When cell voltage approaches the limit, the charging current begins to taper off (Figure 32a). The cell voltage is sensitive to small changes in cell temperature, however, so the limit on charging voltage may be set too high to permit complete charging safely. An alternate approach would be to switch to a lower charging current by lowering the applied voltage (Figure 32b) when the detection system indicates the battery is going into overcharge (Reference 11, page 25).

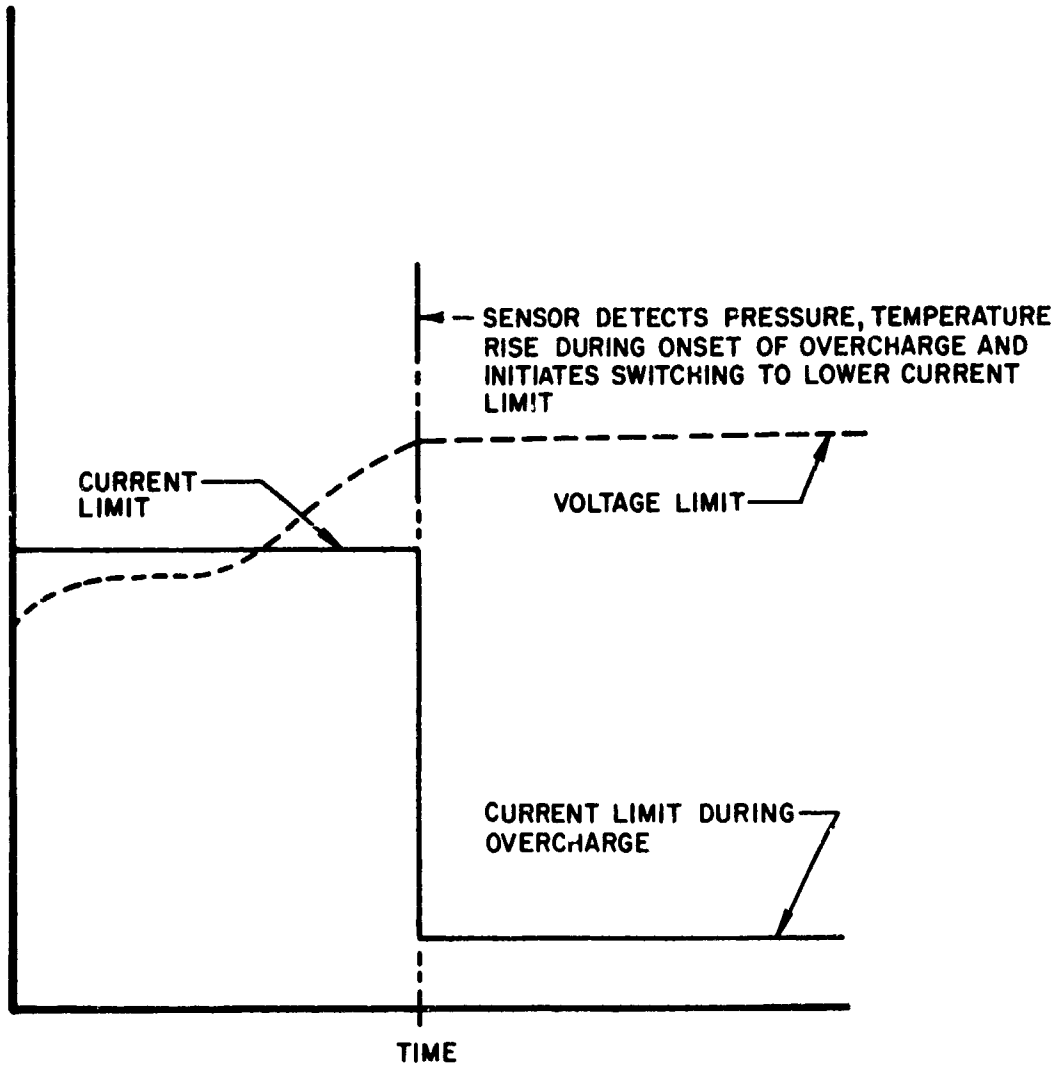


Figure 31. Voltage Limit, Constant Current Charge Control, With Current-Initiated Switchdown

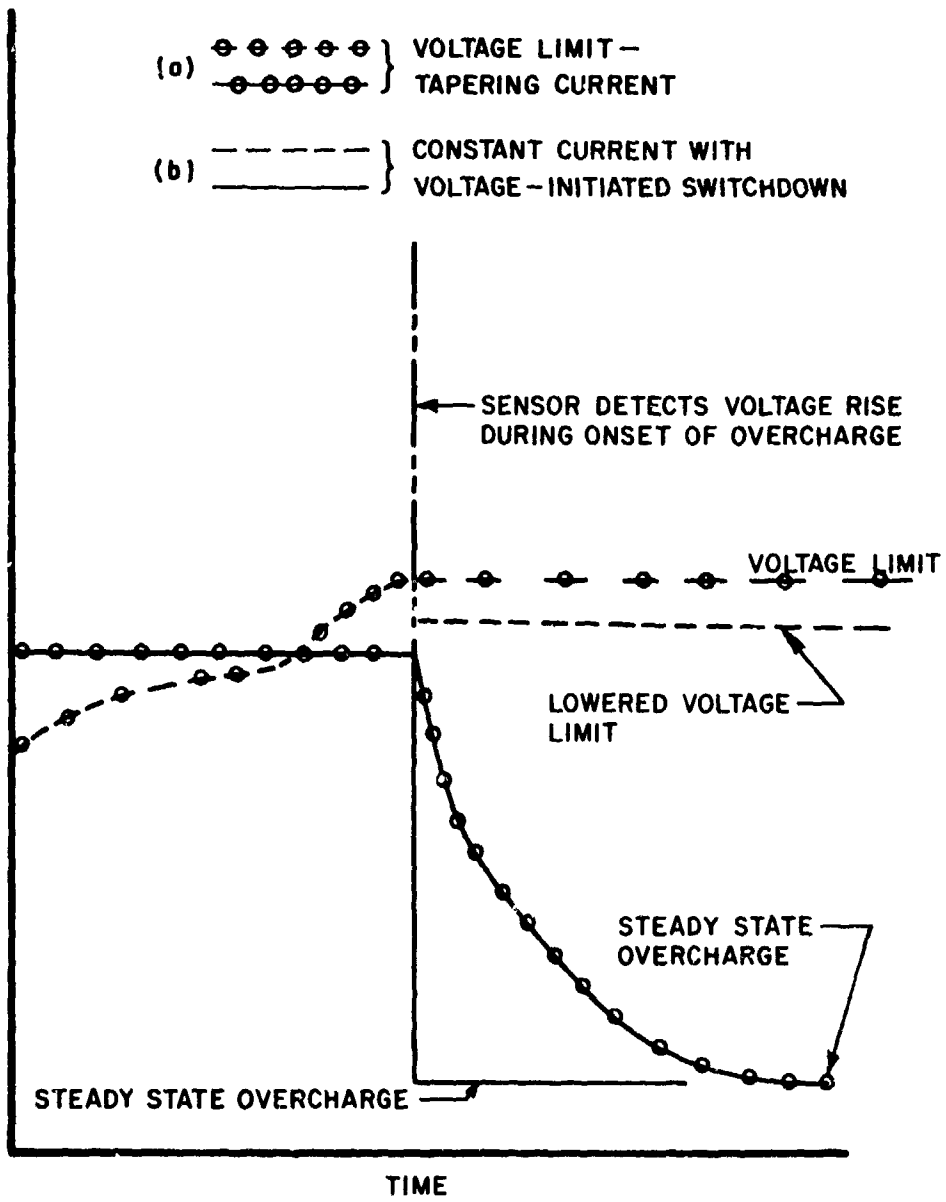


Figure 32. Comparison of Charge Control Methods

(3) Individual Cell Bypassing During Charge. Overcharge might be controlled by bypassing individual cells without affecting the entire battery during the charging cycle. Cells that have been fully charged are bypassed and the remaining cells can use maximum charge current. Thus, if high impedance occurs in one cell, the voltage is limited across this cell while the rest continue to be charged (Reference 3, page 60). A word should be said here about sequential charging. If multiple cell strings are charged in parallel, then the size of the solar panel required to charge these strings is proportional to the charge current. If individual cell strings (a single battery) are charged in series (sequentially), however, all the strings may be charged at the same rate but at a lower current level, thereby reducing the size and weight of the solar array. The charge cycle would show one battery on trickle charge while another is on active charge. In this way the weight of the solar panel required to charge the batteries would be reduced by 40 to 50%. There are offsetting disadvantages to this method. As mentioned before, battery utility is reduced greatly because only about half of the battery power will be available for transient or emergency conditions during any synchronous orbit. Sequential charging appears to offer a total panel weight reduction of up to 15% for an array sized to deliver 2 kw EOL, but this may be overoptimistic; additional switching equipment, cabling, and extra packaging would be required, so the net savings may be about 10 lbs out of 190 lbs total weight for the 2 kw EOL system load conditions at a C/5 charge rate (Reference 3, page 101-103).\* This charging process has been rejected because we believe that the amount of switching required would reduce reliability (Reference 14).

b. Sensing End of Active Charge

Several techniques have been presented to prevent excessive temperature rise and pressure buildup during overcharge, but some reliable way must be employed to detect the onset of overcharge. Several techniques are described briefly below:

(1) Battery Voltage Rise. This method simply uses the battery voltage rise during charging to indicate the state of charge. Unfortunately, the rate of change of voltage is not very great near the end of charge, and it becomes even smaller with increased temperature.

\*At 50 lbs/kw solar panel specific power.

(2) Decreasing Battery Current. If the battery voltage limit method of charge control is used, the point where the charge current begins to taper off can be used to signal overcharge. For Ni-Cd cells this method is not too reliable, however, because the rate of current decrease depends on cell temperature and the selected voltage limit.

(3) Auxiliary Electrode. A third electrode can be used to detect the presence of oxygen in the cell. When oxygen is evolved, this sensor would produce a voltage or current which can be used to activate the charge control circuitry to reduce the charging current. The electrode must have the proper sensitivity, however, or the charging may be stopped before the battery is fully charged; if sensitivity is too low, oxygen pressure may become too high before charging is stopped. For continuous cycling, any excess oxygen evolved before the electrode signals the presence of the gas must be recombined during the discharge cycle to prevent loss of effective charge control. Studies are being made to develop an auxiliary electrode that will promote the oxygen recombination during discharge (Reference 13, page 401-402).

(4) Cell Temperature Rise. Detection of cell temperature rise appears to be a good way to determine end of charge, since temperature begins to rise rapidly as the cell approaches overcharge. The disadvantage of this method is that a change in cell temperature tends to follow a reduction in charge efficiency.

(5) Ampere-Hour Accounting. Data obtained on 90-minute orbits indicate that end of charging may possibly be determined by using a coulometer to count hours put into a battery during charge, since the ratio of  $AH_{in}$  to  $AH_{out}$  during discharge is fairly well known for these orbits. At this time, little data is available for the synchronous orbit cycle.

In summary, a combination of control techniques and charge sensing devices will probably be used to detect the onset of overcharge and limit the charging current. Studies by industry (References 3, page 63; and 15 and 16) indicate that the initial high charge rate will be followed with a low current trickle charge.

### 3. BATTERY/RADIATOR SYSTEM WEIGHT

Heat is radiated from the battery during discharge, and also during overcharge under a high charging current. Some sort of heat transfer mechanism must be provided to dissipate this heat load safely. Simple space radiators and heat pipes have been considered. The heat rate rises rapidly during overcharge, as well as with an increase in charge rate, but the charge rate should not significantly affect radiator design or weight. Efficient charge detection and control devices should switch the battery to trickle charge before the temperature rises significantly. The charge control technique should keep the heat load during overcharge to less than that during discharge; at the worst case, loads should be only slightly higher, so that the weight of the total battery/radiation system would increase by only a few percent. It has been estimated that weight of miscellaneous hardware, shielding, and thermal control will change total weight of the battery/radiator system for a 2 kw load by no more than  $\pm 10\%$ . The greatest fraction of the total system weight is in the battery cells (Reference 3, page 139, 140).

Battery system weight is affected greatly by the depth-of-discharge selected (See Figure 22). Maximum D. O. D. is desirable to minimize weight, but weight savings must be traded off with cell reliability, as shown in Figure 28.

## APPENDIX II

## PROPULSION AND POWER PERFORMANCE CONSTRAINTS

We chose a colloid thruster having multimillipound thrust capability, with a slit or an annular needle ("thick" needle) geometry, specific impulse of 1500 seconds at an overall efficiency of 70% and projected performance improvement up to 2000 seconds\* at 70% efficiency. Colloid capillary needles and thick needles have operated for lifetimes up to 1000 hours at specific impulses from 1000 to 1500 secs. The formation of tar has been a problem with the high thrust density sources, but very little has been observed with the small needles. An Advanced Development Program on the small needles is currently in the Critical Component Development Phase to design, fabricate, and life-test a millipound thrust module for 10,000 hours. More detailed information on colloids can be found in Reference 17.

A cesium bombardment ion thruster was chosen to satisfy multimillipound thrust requirements of 1820 to 8500 secs\*\*, specific impulse, with an overall efficiency of 40% at low Isp and 70% at the high value. Multimillipound thruster sources have operated for thousands of hours; one test was conducted for 8100 hours at 6.7 mlbs, 5000 seconds, at 71% thrust efficiency; the run was terminated when the propellant was exhausted. No Advanced Development work is currently

\*Recent test correlation indicate that current thruster performance determination may be somewhat in error, reducing the actual specific impulse from 1500 to possibly as low as 1200 seconds in some cases at the extraction voltages in the neighborhood of 15 KV. According to the theory of charged particle formation in a NaI/glycerol solution there may be an upper limit to practical Isp operation because of the solubility limit of iodine in glycerin (Reference 18). As the charge-to-mass ratio of the solution droplets is raised (by higher voltages, lower flow rate, etc.) the solubility limit of iodine in glycerol may be reached and gaseous iodine may be evolved or precipitated out. These effects can cause tar formation in the source with resultant decrease in thruster performance and operating stability. Therefore, it may not be possible to operate a slit source at 2000 secs in a uniform and reliable mode, using the above-mentioned propellant.

\*\*Accomplished with two different thruster designs - 1820-5000 secs and 5000-8500 secs (upper limit). This full range requirement occurs only for the ion engine operating on the full power sharing mode at a charge rate of C/10 and  $\Delta V = 635 \text{ ft/sec/yr}$ .

planned for the near future, but a millipound thrust, 2500-sec engine is being developed for use on the NASA/Goddard ATS-F satellite. More detailed information on cesium bombardment ion engines can be found in References 7, 19. The efficiency of ion engine systems vs Isp for multimillipound-size thrusters is shown in Figure 14.

Secondary battery performance was chosen as 8 watt-hrs/lb at 70% depth of discharge (150 lbs/kw); charge rates from C/4 to C/10 were used. A battery ADP will test secondary batteries to meet the objectives of 166 lbs/kw, 2 kw constant power, 7 years operation (88 eclipse periods). The depth of discharge goal is 70% and the temperature constraint is 30-60°F. The prime charge rate will be in the neighborhood of C/4 to C/10, with a trickle charge of about C/40. Current test plans are to charge the battery initially at C/4-C/5 when extra solar power is available, due to sizing for degradation and then at C/10 near end of life (Reference 20). A heat pipe will probably be used in the thermal control system.

For this analysis constant charge rates of C/4 and C/10 were used. Batteries have been tested in synchronous-orbit-type cycling for periods of up to 1000 days, but the parameters of temperature, charge rate, and depth of discharge were varied almost indiscriminately from test to test. Information on projected capability and current performance can be found in References 3 and 21.

Solar cell performance was considered to be 50-100 lbs/kw for advanced flexible roll-up arrays, with 25% degradation after 10 years at synchronous altitude. Solar cell work under an ADP to design a high performance flexible roll-up array, is directed toward achieving a 5-year life goal with 18% degradation. Specific power of the array, including orientation structure and power conditioning weights (additional information on solar cell performance can be found in References 1 and 9), is 110 lbs/kw for a 1.5 array. Projected performance for a 5 kw array is in the neighborhood of 50-75 lbs/kw.

## APPENDIX III

## POSITION OF THE NODES FOR A SYNCHRONOUS EQUATORIAL ORBIT

A synchronous equatorial satellite that is unperturbed will stay over a position on the earth indefinitely because its circular orbital period corresponds to the earth's rotational period of nearly 24 hours. The Earth moves  $0.985^\circ$  per day in its path around the sun, however, so the position of the nodes with respect to the sun-earth line will move accordingly in an east-to-west direction. During the 45-day eclipse season, the nodal points will move about 44 degrees (3 hours), with respect to the Earth-sun line (shadow). Perturbations due to the oblateness of the Earth will cause the nodes to precess approximately 5 degrees per year east to west. This perturbation is negligible in considering the position of the nodes during the 45-day eclipse season, but it should be taken out periodically if precise E-W station keeping is desired (Reference 22). The position of the unperturbed nodes with respect to the Earth's shadow for the eclipse season is shown in Figure 33. During the autumnal equinox, when the eclipse reaches a maximum of 1.2 hours, the descending node (where the satellite crosses the equatorial plane from N to S) is in the shadow; during the vernal equinox, the ascending node is in the shadow.

At the beginning and end of the eclipse seasons, the satellite crosses the equatorial plane at a point  $22^\circ$  (1.5 hours) before and after the midpoint of the eclipse period. This figure shows a scheme for cycling the N/S station-keeping thruster and the battery charging periods on a noninterference, or power-sharing, basis. Because of the relative movement of the nodal points with respect to the Earth's shadow, some type of sensor/clock mechanism is needed to sense the satellite's position in the orbit with respect to the nodal points and the shadow so that thruster operation may be initiated near the nodes. Since no solar power is received during the eclipse, the thruster operating near the nodal point closest to the shadow must be cycled on and off as it passes through the shadow. To facilitate rapid turn on to full thrust after leaving the shadow, several watts of power could be taken from the secondary batteries to keep the thruster and feed

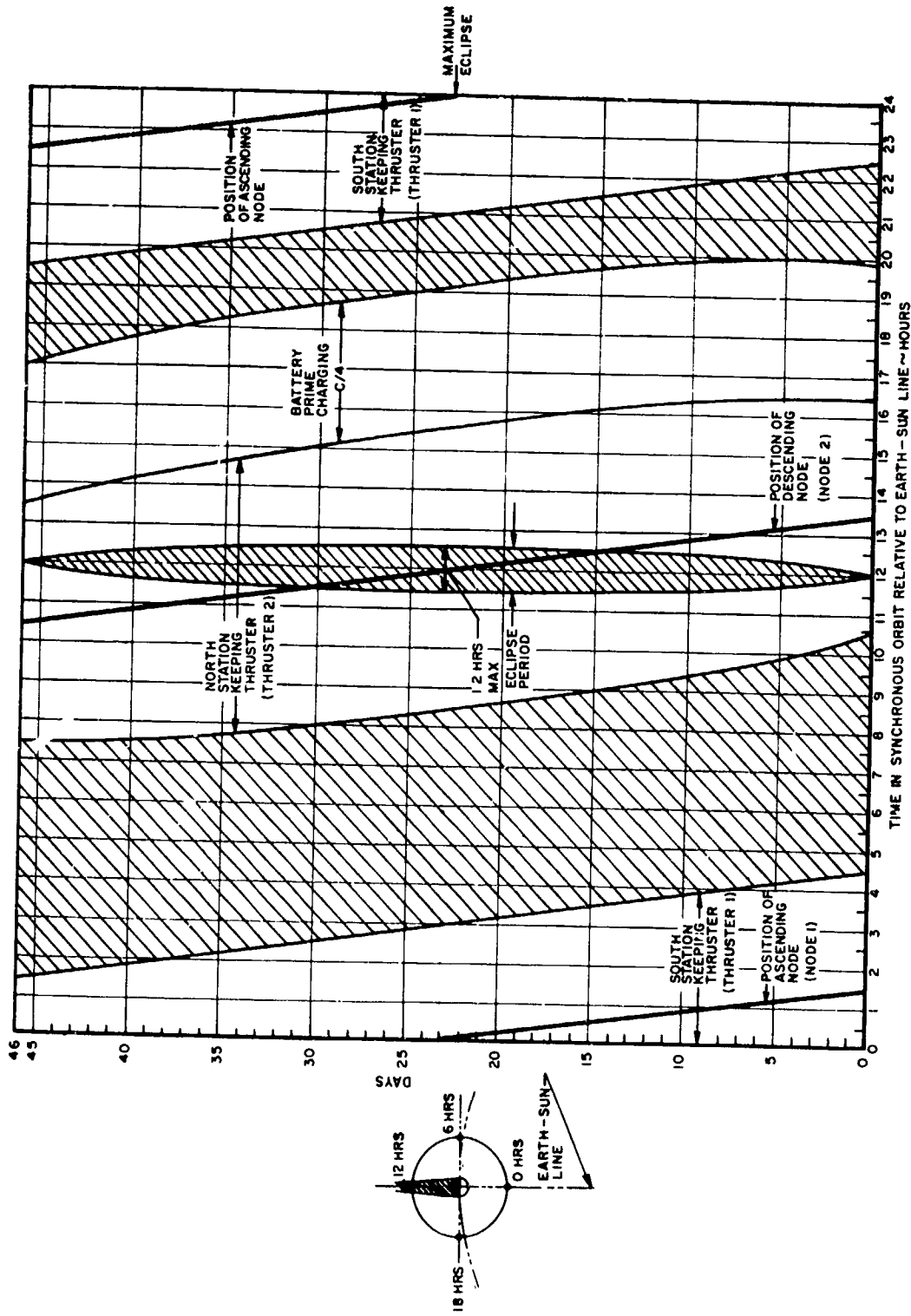


Figure 33. Thruster/ Battery Charging Operating Cycles for Synchronous Equatorial Satellite During 45-Day Autumnal Equinox Season

system at operating temperature.\* As shown in Figure 33, North station-keeping thruster (Thruster 2) at the descending node (Node 2) can operate both before and after the eclipse. The representative thruster cycle is shown to operate three hours on each side of the node; because of the position of Node 2 with respect to the shadow, however, the total time elapsed from start of thruster operation to shut down during the dark time, and start and stop after the shadow varies from 6 to 7.2 hours. The South station-keeping thruster (Thruster 1) can operate  $\pm 3$  hours around Node 1 throughout the 45-day autumnal equinox season. The additional  $\Delta V$  penalty imposed on Thruster 2 because it occasionally begins and ends operation at a maximum of 3.6 hours from the node, instead of 3 hours, is negligible (1% when considering the overall effect on required N/S station keeping for the entire year.) The Thruster 2 cycle varies from 4.5 to 1.5 hours before the shadow, with the remaining time occurring after it emerges from the shadow.

Figure 33 shows the battery charging period occurring immediately after operation of Thruster 2 is terminated. The charge cycle (C/4 charge rate) is shown to begin from 1.5 to 4.5 hours after the satellite leaves the shadow. This charge cycle will not interfere with the operation of Thruster 1. Some sort of clock/timer mechanism will be needed to control thruster operation and battery charging so that the thruster is not turned on during the eclipse and the battery does not begin the high rate of charging until the thrust cycle is over. This device obviously must have a high reliability. Figure 34 shows the power profile for a charge rate of C/4 during the autumnal equinox season, when the eclipse season is maximum -- 1.2 hours. Figure 35 shows a profile for a charge rate of C/10.

---

\*Because the batteries are sized for maximum dark time energy output over 1.2 hours, it may be possible to use some of the excess stored energy in the batteries to operate the thruster during the portion of the eclipse season when the shadow time is somewhat less than 1.2 hours. This however, was not considered in this study.

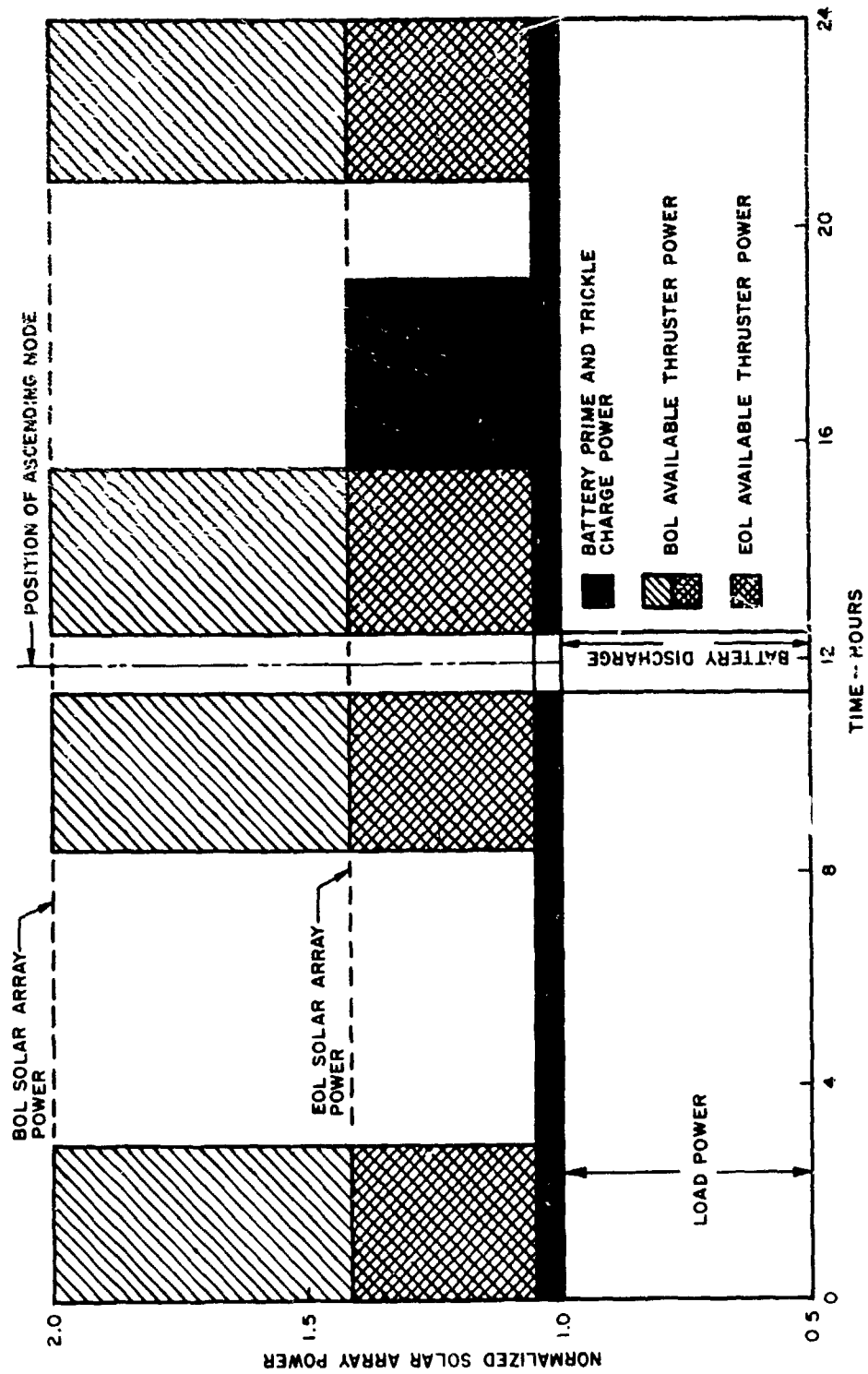


Figure 34. Typical Power Profile for Synchronous Equatorial Satellite With C/4 Battery Charge Rate, During Autumnal Equinox

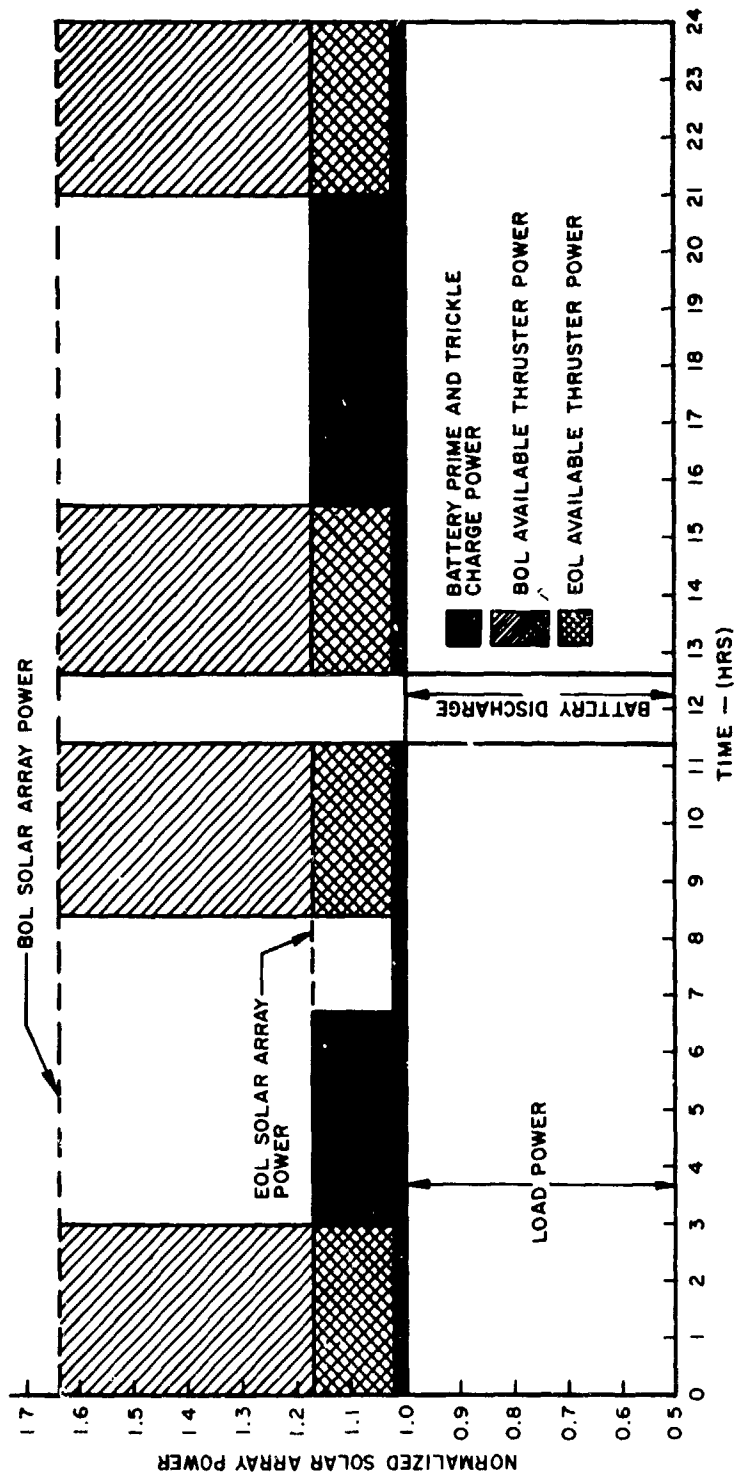


Figure 35. Typical Power Profile for Synchronous Equatorial Satellite With C/10 Battery Charge Rate During Autumnal Equinox

APPENDIX IV  
DIGITAL COMPUTER PROGRAM  
FOR POWER-SHARING ANALYSES

14 SAM ----- CDC 5600 FIN V3.0-2243 OPT=1 047

```

PROGRAM SAM (INPUT,OUTPUT,TAPE 5 = INPUT, TAPE 6 = OUTPUT.)
REAL L , NOC , ND , NSDV , NC , MFI , MFC , MKWHL , MAHL , IYNS ,
1 IYNSI , IYNSC , ISPI(4) , ISPC(5) , ISPC1(4) , ISPC2(4) , NI(4) ,
2 NII(5) , IREP
DIMENSION Y(4) , X(4) , TASP(4) , HI(5) , TPI(4) ,
1 TPC1(4) , TPC2(4) , COEF(4)
2 , FL(3) , FSATH(3) , FBCHR(3) , FBTCHR(3) , FNSDV(3) , FMFC(3) , FNOC(3)
DATA (NII(I) , I = 1,5 ) / .4) , .55 , .65 , .70 , .75 /
DATA ( HI(I) , I = 1,5 ) / 3500. , 4500. , 5500. , 7000. , 8500. /
DATA (COEF(I) , I = 1,4 ) / 1. , 2. , 2. , 5. /
DATA (FL ( I) , I=1,3) / 10. , 7. , 2.5 /
DATA (FSATH(I) , I=1,3) / 10000. , 7100. , 2500. /
DATA (FNSDV(I) , I=1,3) / 157. , 300. , 635. /
DATA (FBCHR(I) , I=1,3) / 4. , 10. , 20. /
DATA (FBTCHR(I) , I=1,3) / 40. , 50. , 50. /
DATA (FNOC(I) , I=1,3) / 1.25 , 1.3 , 1.35 /
DATA (FMFC(I) , I=1,3) / 1. , 1. , 1. /

```

```

G = 32.2
T = 10.
DOD = .70
ND = .7
NSDV = 635.
Y(1) = .12
Y(2) = .175
Y(3) = .21
Y(4) = .25

```

```

NC = .70
PTF = 1.07
MFI = 1.0
REPOV = 312.
TREP = .040
ISREI = 5000.
ISREC = 1500.
ALPHA = 50.
WHLB = 8.

```

```

DO 200 I1=1,3
L = FL(I1)
SATH = FSATH(I1)
DO 200 I2=1,3
NSDV = FNSDV(I2)
DO 200 I3=1,3
BCHR = FBCHR(I3)
BTCHR = FBTCHR(I3)
NOC = FNOC(I3)
MFC = FMFC(I3)
IF ( I2 .EQ. 3 ) MFC = .95

```

-----  
 IN SAN ----- COC 6600 FTN V3.0-P243 OPT=1-34/3

-----  
 MKWHL = L\*1.2  
 9CWHL = MKWHL/DOD  
 MAHL = BCWHL\*1.E3 / 42.  
 BCHI = MAHL / BCHR  
 BTCHI = MAHL / BTCHR  
 BCHP = BCHI\* 42. \* 1.E-3  
 BTCHP = BTCHI\*42. \* 1.E-3  
 TBCHP = BCHP - BTCHP  
 BCHT = DOD\*NOG \* MAHL / BCHI  
 ASCHB = L + BCHP  
 SABOL = ASCHB / NO \*1.05  
 -----

-----  
 IYNS = NSOV\*SATH / G  
 IYNSI = IYNS \* 1.11\*MFI  
 IYNSC = IYNS \* 1.02 \* MFC  
 FNSI = IYNSI / ( 3.17\* 1.E7 \* .50 )  
 FNSC = IYNSC / ( 3.17\* 1.E7 \* .25 )  
 EPBOL = SABOL - L - BTCHP  
 DO 10 N = 1,4  
 10 X(N) = ( 1. - NO - Y(N) ) / ( 1. - NO )  
 -----

-----  
 DO 50 N=1,4  
 TASP(N) = TBCHP + X(N) \* EPBOL  
 DO 40 I=1,5  
 ISPI(N) = TASP(N)\*45.9\*NII(I) / FNSI \$ NI(N)=NII(I)  
 IF ( ISPI(N) .LE. HI(I) ) GO TO 50  
 40 CONTINUE  
 ISPI(N) = 8500.  
 50 CONTINUE  
 WNSI = 0.  
 DO 60 I=1,4  
 60 WNSI = WNSI + COEF(I) / ISPI(I)  
 WNSI = WNSI \* PTF \* IYNSI  
 AISPI = IYNSI \* 10. \* PTF / WNSI  
 -----

-----  
 DO 70 N=1,4  
 ISPC(N) = (45.9\*NC \* TASP(N) ) / FNSC  
 IF ( ISPC(N) .GE. 2000. ) GO TO 69  
 ISPC1(N) = 1500.  
 ISPC2(N) = ISPC(N)  
 GO TO 70  
 69 ISPC1(N) = 1500.  
 ISPC2(N) = 2000.  
 70 CONTINUE  
 WNSC1 = 0.  
 WNSC2 = 0.  
 DO 75 N=1,4  
 WNSC1 = WNSC1 + COEF(N) / ISPC1(N)  
 -----

3

SAM CDC 6000 FTN V3.0-P243 OPT=1 04/30/71

```

-----
WNSC2 = WNSC2 + COEF(N) / ISPC2(N)
5 CONTINUE
WNSC1 = WNSC1 * PTF * IYNCS
WNSC2 = WNSC2 * PTF * IYNCS
AISC1 = IYNCS * 10. * PTF / WNSC1
AISC2 = IYNCS * 10. * PTF / WNSC2
DO 80 N=1,4
TPI(N) = (FNSI*ISPI(N)) / (45.9 * NI(N))
TPC1(N) = (FNCS*ISPC1(N)) / (45.9 * NC)
0 TPC2(N) = (FNCS * ISPC2(N)) / (45.9 * NC)
-----

IREP = (REPDV*SATH) / G
WREPI = (IREP*PTF) / ISREI
WREPC = (IREP*PTF) / ISREC
WSP = SABOL * ALPHA
WSB = (BCWHL * 1.0E3) / WHLB
-----

WRITE(6,411) L,SATH,NSDV,BCHR,BTCHR,NOC,MFC
111 FORMAT(1H1,*L=*,E14.4,2X,*SATH=*,E14.4,2X,*NSDV=*,E14.4,2X,*BCHR=*
1 ,E14.4,2X /1X,*BTCHR=*,E14.4,2X,*NOC=*,E14.4,2X,*MFC=*,E14.4)
WRITE(6,101) MKWHL,BCWHL,MAHL,BCHI,BTCHI,BCHP,
1 BTCHP,TBCHP,BCHT,ASCHB,SABOL
-----

101 FORMAT(1H ,*MKWHL* / (1X,E20.6))
WRITE(6,104) IYNS,IYNSI,IYNCS,FNSI,FNCS,EPPOL
104 FORMAT(1H0,*IYNS* / ( E20.6))
WRITE(6,99) (X(N),N=1,4)
39 FORMAT(1H0,*X* / ( E20.6))
WRITE(6,106) (TASP(N),ISPI(N),NI(N),N=1,4) ,AISPI
106 FORMAT(1H ,*TASP* . 20X,*ISPI*,20X,*NI*,
1 / ( 3E20.6))
WRITE(6,109) (ISPC(N),TPI(N),TPC1(N),TPC2(N),N=1,4)
109 FORMAT(1H ,*ISPC*,20X,*TPI*,20X,*TPC1*,20X,*TPC2*,
1 / ( . 4E20.6))
WRITE(6,111) ISPC1,ISPC2,AISC1,AISC2
111 FORMAT(1H ,*ISPC1* / (1X,E20.6))
WRITE(6,114) WNSI,WNSC1,WNSC2,IREP,WREPI,
1 WREPC,WSP,WSB
114 FORMAT(1H ,*WNSI* / (1X,E20.6))
200 CONTINUE
STOP
END
-----

```

REFERENCES

1. Private communications with TRW systems.
2. Private communications with personnel of AFAPL/POE-2, Energy Conversion Branch and AFAPL IPOP-3, Laser and Aircraft Power Branch
3. Two Kilowatt Long Life Battery, AFAPL-TR-70-31, TRW Systems, JNC, Redondo Beach, Calif, Sept 1970.
4. R. A. Benson, D. S. Goldin, Missions and Spacecraft Interface Requirements for Secondary Propulsion Subsystems and Their Impact on Colloid Systems, TRW Systems, May 1969, page 4-6.
5. G.d. Munz, J. Oberstone, Propulsion, Systems for Advanced Geosynchronous Satellites, Aerospace Corporation, SAMSO-TR-70-171, May 1970.
6. J. H. Molitor, Hughes Research Laboratories, Application of Ion Thrust Motors in Attitude and Position Control of Satellites, presented at the technical meeting of the Combustion and Propulsion Panel of AGARD, Athens, Greece, July 15-17, 1963, page 8-9.
7. R. Shattuck, Electro Optical System, Auxiliary Propulsion Survey, Part I, Electric Thrusters Survey, AFAPL-TR-68-67, Sept 1968.
8. Private correspondence from the Rand Corporation, Santa Monica, Calif
9. Flexible Rolled Up Solar Array, 10th Quarterly Report, F33608-C-1676 Hughes Aircraft Company, El Segundo, Calif, June 1971.
10. Private communications with personnel of AFAPL IPOP-3, Laser and Aircraft Power Branch
11. Paul Bauer, Batteries for Space Power Systems, written under contract for NASA by TRW Systems, Redondo Beach Calif, 1968.
12. K. E. Prell SSE, R. C. Shain, F. E. Betz, Parametric Charge Studies for Aerospace Nickel - Cadmium Batteries, Gulton Industries, Inc, Metuchen, N. J, paper presented at 6th International Power Source Symposium held at Brighton, Sussex, 23-25 Sept 1968.
13. W. N. Carson, Jr, R. L. Hadley, Rapid Recharging of Nickel - Cadmium Batteries, General Electric Co, paper presented at 6th International Power Source Symposium held at Brighton, Sussex, 23-25 Sept 1968, page 393.
14. Private communications with personnel of AFAPL (POE-1).
15. Private communications with personnel of Hughes Space System Division, El Segundo, Calif.

REFERENCES (Contd)

16. Private communications with personnel of Lockheed Missiles and Space Company, Sunnyvale, Calif.
17. Charged Droplet Electrostatic Thruster Systems, AFAPL-TR-70-31, TRW Systems, Redondo Beach, Calif, June 1970.
18. Exploratory Development of Advanced Colloid Thrusters, TRW Systems, Redondo Beach Calif, monthly report #8 of Contract F33615-70-C-140E, Oct 1970, page 25-26.
19. E. James, et al, A One Millipound Cesium Ion Thruster System, Electro Optical Systems, Pasadena, Calif, AIAA paper no 70-1149 presented at AIAA 8th Electric Propulsion Conference at Stanford, Calif Aug 31 - Sept 2, 1970.
20. Private communications with Dr. Willard Scott, TRW Systems Inc, Redondo Beach, Calif.
21. Evaluation Program for Secondary Spacecraft Cells; Synchronous Orbit Testing of 6.0 Ampere - Hour Sealed Nickel - Cadmium Cells Manufactured by General Electric Co - prepared for Goddard Space Flight Center Contract W12,397 Quality Evaluation Laboratory, Nad Crade, Indiana, Aug 1970.
22. Space Planners Guide, USAF/AFSC, page II-51, July 1965.